Author(s)	Graham, Robert J.; Lloyd, Theodore L.
Title	Frequency response investigation of a second order serve with backlash
Publisher	Monterey, California. Naval Postgraduate School
Issue Date	1962
URL	http://hdl.handle.net/10945/26562

FREQUENCY RESPONSE INVESTIGATION OF A
SECOND ORDER SERVO WITH BACKLASH

ROBERT J. GRAHAM
and
THEODORE L. LLOYD, JR.

FREQUENCY RESPONSE INVESTIGATION

OF A

SECOND ORDER SERVO

WITH

BACKLASH

* * * * * *

Robert J. Graham

and

Theodore L. Lloyd, Jr.

FREQUENCY RESPONSE INVESTIGATION

OF A

SECOND ORDER SERVO

WITH

BACKLASH

by

Robert J. Graham

Lieutenant Colonel, United States Marine Corps

and

Theodore L. Lloyd, Jr.

Lieutenant, United States Navy

Submitted in partial fulfillment of
the requirements for the degree of

MASTER OF SCIENCE
IN
ELECTRICAL ENGINEERING

United States Naval Postgraduate School
Monterey, California

1 9 6 2

FREQUENCY RESPONSE INVESTIGATION

OF A SECOND ORDER SERVO

WITH BACKLASH

by

Robert J. Graham

and

Theodore L. Lloyd, Jr.

This work is accepted as fulfilling
the thesis requirements for the degree of

MASTER OF SCIENCE

IN

ELECTRICAL ENGINEERING

from the

United States Naval Postgraduate School

ABSTRACT

The frequency response was determined for a second order servo-
mechanism with backlash in the system. Frequency response for sinu-
soidal inputs were obtained by digital computer solutions of the
equations of motion of the system which had inertia and viscous
friction on both sides of the gear train. System parameters included
input amplitude, magnitude of backlash, damping ratio and resilience
of the gear teeth.

The Control Data Corporation 1604 Computer was utilized and
Fortran programming was employed.

Results show the effects of the amount of backlash and the
gear material resilience on the output to input ratios. The exist-
ence of sub-harmonic resonance was found with large values of back-
lash.

TABLE OF CONTENTS

LIST OF ILLUSTRATIONS

TABLE OF SYMBOLS

		Program Mnemonic
Input position	Θ_R	FORCE
Output position (motor & load combined)	Θ_c	THEC
Output velocity (motor & load combined)	$\dot{\Theta}_c$	THECD
Output acceleration (" " ")	$\ddot{\Theta}_c$	THECDD
Friction of motor	f_M	FM
Friction of load	f_L	FL
Inertia of motor	J_M	DM
Inertia of load	J_L	DL
Gear ratio of gear train	ρ	RHO
Gain of system	K	GC
Damping ratio	$\mathcal{J}$	ZETA
Undamped natural frequency of system	ω_n	WN
Amplitude of sinusoidal input	A	A
Frequency of sinusoidal input	ω	W
Position of motor	Θ_M	THEM
Velocity of motor	$\dot{\Theta}_M$	THEMD
Acceleration of motor	$\ddot{\Theta}_M$	THEMDD
Position of load	Θ_L	THEL
Velocity of load	$\dot{\Theta}_L$	THELD
Acceleration of load	$\ddot{\Theta}_L$	THELDD
Phase plane slope of combined motor and load	N_c	SLOPEC
Phase plane slope of load separated	N_L	SLOPEL

Magnitude of backlash	$\triangle$	BL
Time	t	T
Integration interval	Δt	TINT
Coefficient of restitution of gear teeth	e	E
Motor velocity after bounce	$\dot{\theta}_M'$	BOMVEL
Load velocity after bounce	$\dot{\theta}_L'$	BOLVEL
Problem time for 5 time constants (linear)	5τ	DELAY
Number which controls computing time after five time constants	-	CYC
Problem computing time after 5τ	-	FINI
Total friction referred to motor	f_T	
Ratio of $|\theta_c|/A$ at resonance	M_p	
Ratio of $|\theta_c|/A$	M	
Relative backlash	$A/\triangle$	

1. BACKGROUND AND INTRODUCTION

Most servomechanisms have a mechanical connection between the driving components and the driven or positioning unit. Usually this connection is a gear train which, in most practical cases, has a finite amount of backlash in the gearing mechanism. This inherently renders the servo system non-linear and requires analysis techniques which are based on approximations or which necessitate use of laborious graphical methods which may rely on simplifying assumptions. The backlash between the gear teeth cannot always be eliminated without possibly introducing other, perhaps less desirable effects such as coulomb friction and/or increased viscous friction. Manufacturing costs may also prohibit consideration of gears with no backlash.

The relative distributions of viscous friction and inertia on each side of the gearing have direct effects on the behavior of the load. Graphical phase plane and analog simulation analysis techniques do not readily adapt to practical consideration and adjustment of these distributions. Also, they cannot handle the case of non-plastic impact of the gear teeth. This has led to the solution of this problem by the use of digital computers.

Several investigations have been made of second order servo behavior using the digital computer at the U. S. Naval Postgraduate School. These include, limit cycle investigation by New for plastic impact (Ref. 1) and by Anderson and Luckett for plastic and elastic impact (Ref. 2), and a transient response investigation for plastic impact by Andrews and Kelley (Ref. 3).

1

This thesis extends the coverage of this problem to a steady-state frequency response investigation, with both plastic and elastic impact, for a periodic (sinusoidal) input of varying frequency and amplitude. The general approach to the investigation was similar to that used by Anderson and Luckett. The equations of motion of the system were normalized so behavior would be independent of the undamped natural frequency of the system. The parameters inertia, viscous friction, elastic "bounce" coefficient and damping ratio were in the same ranges of values used by Anderson and Luckett so that a correlation of results could be made if desired.

Computations were made on a CDC 1604 digital computer using a Fortran System program which had definite advantages over the machine language programs used in the previous investigations mentioned above. Solution of the system equations was based on the phase plane approach as to whether the system was operating combined or separated. Even though the system was normalized, the computer program was made general to permit extension of the values of the parameters if desirable.

This thesis includes investigation of the effects of the amount of backlash, the amplitude of the periodic input and the amount of system damping for both plastic and elastic impact of the gear teeth. The only non-linearity considered was backlash.

The total system was piecewise linear in that one linear differential equation described the motion of the system when the driving motor was combined with the load and two different linear differential equations described the separated motions of the motor and load.

2

Boundary conditions for the differential equations were based on phase plane slopes and on equations based on the laws of conservation of energy and momentum which were related to whether gear contact was plastic or elastic.

The original intention was to determine the effects of different distributions of inertia and viscous friction between the driving unit (motor) and the driven unit (load). However, because of the great amount of digital computer operating time required, it was necessary to confine the investigation to one ratio of inertias and one ratio of frictions.

Results from the digital computer calculations provided data from which the magnitude of the output and the phase relation between input and output could both be determined. This thesis is concerned only with the magnitude of the output as compared with amplitude of the input sinusoid.

Special effects or phenomena such as jump resonance and sub-harmonic resonance, which are known to exist under certain conditions, were looked for in the course of the investigation.

In the following sections the system equations are developed and the evolution of the computer program is described. A print of one version of the Fortran language computer program and the computer solution flow chart are included as appendices.

3

2. SYSTEM DESCRIPTION AND DEVELOPMENT OF EQUATIONS

2.1 Description of System

For the purpose of this investigation, a second order system was chosen. The block diagram of the system is as follows:
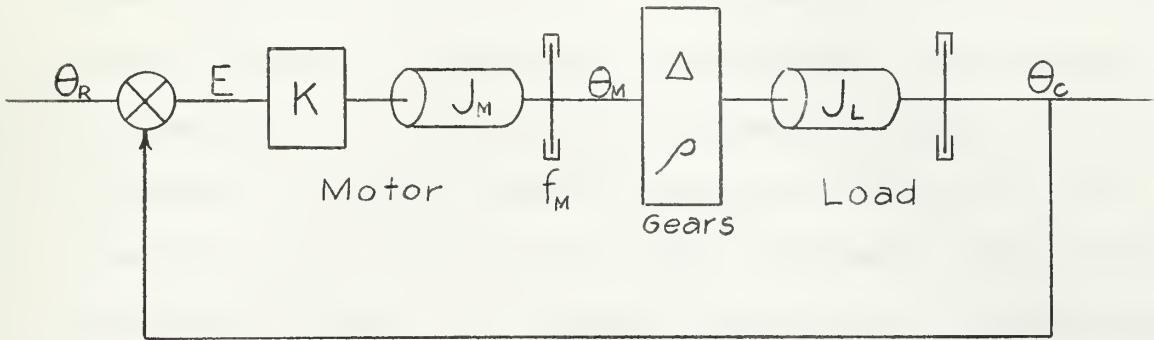
Fig. 2-1

This system is the same system that was reported by Anderson and Luckett in Ref. 2. Except for the non-linearity, the system is a simple second order servomechanism. There is only one non-linearity present, and that is backlash. The backlash is present in the gear train which separates the motor from the load. The effect of the backlash is to allow movement of the load and/or the motor independent of the movement of the other, so long as this movement does not exceed the amount of backlash. Also included as part of the gear train is the gear ratio; however, this has no special effect on the system other than is normally expected.

Separated by the backlash is the motor inertia and friction and the load inertia and friction. The distribution of these quantities cannot be changed in the describing equations of the system due to

4

the backlash. In the linear case, the inertia and friction can be lumped on either side of the gear train without affecting the system operation, but this cannot be done when there is backlash present.

The motion of the system can be described by a combination of three linear differential equations. When the gear teeth are touching, a single differential equation describes the motion. Once the gear teeth separate, one linear differential equation describes the motion of the motor, and another describes the motion of the load. Upon recombining of the gear teeth, the single differential equation again describes the motion. At the instant of separation or recombination, the appropriate differential equations have as initial conditions the last values of the equation which described the motion prior to the separation or recombination. The change over from one describing equation to the pair of equations and vice versa will be discussed further in the equation development section.

2.2 Assumptions

Prior to developing the equations which describe the motion of the system under consideration, the assumptions which have been made will be presented. These assumptions are essentially those made in Ref. 2 and are repeated for convenience but with some modification.

The following assumptions were made:

1. The gear teeth were initially in contact, and the initial conditions of the system were all equal to zero.

2. Plastic deformation of the gear teeth during steady state con-

tact or on impact and any torsional deformations of driving shafts are negligible.

3. The inertias of the gears and drive shafts are considered as part of the load or motor inertia depending on their attachment in the system.

4. The law of conservation of energy is completely satisfied in the perfect elastic case, and the law of conservation of momentum is satisfied in the imperfect elastic cases including the plastic case. When only the law of conservation of momentum is required to be satisfied, the energy lost by the system is dissipated in the form of heat by infinitesimal deformations of the gear teeth.

5. The gear teeth are in contact only instantaneously during impact for all cases except the plastic case, and the impulse torques of drive, friction, bearing supports, etc., are zero during impact.

6. The coefficient of restitution of the two opposing gear teeth is the same or can be described by an equivalent coefficient if the gear teeth are of unequal coefficients.

7. Backlash is assumed to be equal at all points on the gear circumference, and the backlash is measured at the output shaft.

2.3 Equation Development

From Fig. 2-1, the error signal, E, is the driving signal. This is equal to:

6

$$E = \Theta_R - \Theta_c \qquad (2\text{-}1)$$

The torque developed by the motor, T_M, is equal to:

$$T_M = KE = K\left(\Theta_R - \Theta_c\right) \qquad (2\text{-}2)$$

Equations (2-1) and (2-2) are true when the load and motor are combined and when they are separated.

The load torque, T_L, is:

$$T_L = J_L \ddot{\Theta}_c + f_L \dot{\Theta}_c \qquad (2\text{-}3)$$

When the load and motor are combined, the load torque when referred to the motor side of the gear train is:

$$T_{LM} = \rho T_L = \rho\left(J_L \ddot{\Theta}_c + f_L \dot{\Theta}_c\right) \qquad (2\text{-}4)$$

The forward or positive direction of the system is defined to be when:

$$\Theta_c = \rho \Theta_M \qquad (2\text{-}5)$$

and the backward or negative direction when:

$$\Theta_c = \rho \Theta_M + \Delta \qquad (2\text{-}6)$$

By differentiating either equation (2-5) or (2-6) with respect to time yields the same results. These are:

7

$$\dot{\theta}_c = \rho\, \dot{\theta}_M \qquad\qquad (2\text{-}7)$$

and

$$\ddot{\theta}_c = \rho\, \ddot{\theta}_M \qquad\qquad (2\text{-}8)$$

Substituting equations, (2-7) and (2-8), into equation (2-4)
yields after rearranging:

$$T_{LM} = \rho^2 \left(J_L\, \ddot{\theta}_M + f_L\, \dot{\theta}_M \right) \qquad\qquad (2\text{-}9)$$

The driving torque of the motor must equal the load torque referred to
the motor side (combined system only) and the load torque of the motor
itself.

$$T_M = J_M\, \ddot{\theta}_M + f_M\, \dot{\theta}_M + T_{LM} \qquad\qquad (2\text{-}10)$$

Substitution of equations (2-1), (2-7), (2-8), and (2-9) into (2-10)
after simplifying gives:

$$\ddot{\theta}_c + \frac{\left(f_M + \rho^2 f_L \right)}{\left(J_M + \rho^2 J_L \right)}\, \dot{\theta}_c + \frac{K\rho}{\left(J_M + \rho^2 J_L \right)}\, \theta_c = \frac{K\rho}{\left(J_M + \rho^2 J_L \right)}\, \theta_R \qquad (2\text{-}11)$$

Rewriting equation (2-11)

$$\ddot{\theta}_c + 2\mathcal{J}\omega_n\, \dot{\theta}_c + \omega_n^2\, \theta_c = \omega_n^2\, \theta_R \qquad\qquad (2\text{-}12)$$

where

$$\omega_n^2 = \frac{K\rho}{J_M + \rho^2 J_L} \tag{2-13}$$

and

$$2\mathfrak{J}\omega_n = \frac{f_M + \rho^2 f_L}{J_M + \rho^2 J_L} \tag{2-14}$$

Equation (2-12), therefore, defines the motion of the system when the gear teeth are combined.

Whenever the gear teeth are separated, there is no driving force on the load, and its motion is defined by the following equation:

$$\ddot{\Theta}_L + \frac{f_L}{J_L}\dot{\Theta}_L = 0 \tag{2-15}$$

To be noted at this point is the change in notation for the load. In order to distinguish between combined and separated operation, the subscript C or L is used respectively for the output.

Combined operation:

      Output position   - Θ_C

      Output velocity   - $\dot{\Theta}_C$

      Output acceleration - $\ddot{\Theta}_C$

Separated operation:

      Output position   - Θ_L

      Output velocity   - $\dot{\Theta}_L$

      Output acceleration - $\ddot{\Theta}_L$

Although this convention in notation was adopted, it should be remembered that the same quantity is described by two different symbols, depending on whether the system is combined or not.

By the gear teeth being separated, the load torque is not reflected back to the motor side of the gear train. Therefore, equation (2-10) reduces to:

$$T_M = J_M \ddot{\Theta}_M + f_M \dot{\Theta}_M \qquad (2\text{-}16)$$

or by substituting equation (2-2) into (2-16) and after rearranging reduces to:

$$\ddot{\Theta}_M + \frac{f_M}{J_M} \dot{\Theta}_M + \frac{K}{J_M} \Theta_c = \frac{K}{J_M} \Theta_R \qquad (2\text{-}17)$$

Since this investigation is directed towards the frequency response of the system, the forcing function is:

$$\Theta_R = A \sin \omega t \qquad (2\text{-}18)$$

If all angular frequencies are divided by the undamped natural angular frequency, ω_n, this effectively is the same as setting ω_n equal to 1. By this normalization, the angular frequency in equation (2-18) is really ω/ω_n. Therefore, the results are applicable to any simple second order system having any natural frequency ω_n, if the forcing function angular frequency is multiplied by the ω_n of that system.

Equation (2-12) describes the motion of the system when the gear teeth are combined. Equations (2-15) and (2-17) describe the motion of the load and motor respectively when the gear teeth are separated.

10

Left to be determined now is the instant when separation or combination occurs.

Use of phase plane analysis is necessary to determine the instant of separation when the gear teeth are combined. By using velocity and position coordinates for the phase plane, the slope of a trajectory is:

$$N = \frac{d\dot{\theta}}{d\theta} \qquad (2\text{-}19)$$

and specifically for the combined system:

$$N_c = \frac{d\dot{\theta}_c}{d\theta_c} = \frac{\ddot{\theta}_c}{\dot{\theta}_c} \qquad (2\text{-}20)$$

With proper manipulation of equation (2-12), the following obtains:

$$N_c = \frac{\omega_n^2\, \theta_R - \omega_n^2\, \theta_c - 2\mathcal{J}\omega_n\, \dot{\theta}_c}{\dot{\theta}_c} \qquad (2\text{-}21)$$

Using similar techniques to find the load alone slope on the phase trajectory from equation (2-15) yields:

$$N_L = -\frac{f_L}{J_L} \qquad (2\text{-}22)$$

Assuming that the system is combined, it will stay combined as long as the magnitude of the load alone trajectory slope is greater than the magnitude of the combined trajectory slope. Symbolically, the system will remain combined so long as the following is true:

11

$$|N_L| > |N_C| \qquad\qquad (2\text{-}23)$$

Separation occurs when the combined trajectory slope equals the load alone trajectory. This, therefore, is the criterion to be satisfied for transferring the motion description of the system from equation (2-12) to equations (2-15) and (2-17).

For the system to recombine after separation, the gear teeth must come into contact with such velocities that they do not bounce apart in the elastic case. To recombine in the plastic case, the gear teeth merely must come into contact.

In the general case, two criterion must be satisfied for the load to recombine with the motor. These are:

1. The gear teeth must touch.

2. The velocities of the load and motor must be such that they are equal after impact. (Elastic case only)

Unless equation (2-5) or (2-6) is true, the gear teeth cannot be in contact. Therefore, when either equation (2-5) or (2-6) is satisfied, the gear teeth have come into contact. In making this test, however, it must be remembered that θ_L is actually used in place of θ_C in equations (2-5) and (2-6). It is re-emphasized that these symbols actually represent the same quantity but are obtained by solving different equations.

If the impact is plastic, the gear teeth will stay together. However, in the elastic case, they do not necessarily have to remain in

12

contact. During impact, the law of conservation of momentum must be satisfied; and after impact, the velocity of the load and motor must be the same for the teeth to remain in contact. By using the law of conservation of momentum, the respective velocities can be determined.

In Ref. 2, the coefficient of restitution was defined. This is:

$$e = -\frac{\left(\rho\dot{\theta}_M' - \dot{\theta}_L'\right)}{\left(\rho\dot{\theta}_M - \dot{\theta}_L\right)} \tag{2-24}$$

or rearranging:

$$\dot{\theta}_M' = \frac{\dot{\theta}_L' - e\left(\rho\dot{\theta}_M - \dot{\theta}_L\right)}{\rho} \tag{2-24A}$$

where the primed terms represent the respective velocities after impact. To satisfy the conservation of mementum law:

$$\frac{J_M}{\rho J_L}\left(\dot{\theta}_M - \dot{\theta}_M'\right) = \left(\dot{\theta}_L' - \dot{\theta}_L\right) \tag{2-25}$$

must be true. To be noted, equation (2-25) is independent of the coefficient of restitution.

Solving equation (2-24) for $\dot{\theta}_M'$, gives equation (2-24A); and substituting the result into equation (2-25), the following expression for $\dot{\theta}_L'$ obtains:

$$\dot{\theta}_L' = \frac{J_M}{\left(J_M + \rho^2 J_L\right)}\left[\rho\dot{\theta}_M\left(e+1\right) + \dot{\theta}_c\left(\frac{\rho^2 J_L}{J_M} - e\right)\right] \tag{2-26}$$

13

If the gear teeth have come into contact, equations (2-26) and (2-24A) can be solved for $\dot{\Theta}_L'$ and $\dot{\Theta}_M'$ respectively. Unless $\dot{\Theta}_L' = \dot{\Theta}_M'$, the gear teeth will not remain together.

In summary, assuming that the system starts in the positive direction from zero with the gear teeth in contact, the operation is as follows:

1. Equation (2-12) defines the motion of the system until equation (2-23) is no longer true.

2. Once equation (2-23) is no longer true, equations (2-15) and (2-17) describe the motion, taking as their initial values the terminal values of (2-12). In general, the direction of the system must be determined so that the proper value for Θ_M can be used to initialize equation (2-17). If $\dot{\Theta}_c$ is positive, equation (2-5) applies. If $\dot{\Theta}_c$ is negative, equation (2-6) applies. In transferring from equation (2-12) to (2-15), $\Theta_L = \Theta_c$.

3. During separated operation, recontact is determined from equation (2-5) or (2-6).

4. In the event of recontact, equations (2-26) and (2-24A) are used to determine if bounce occurs. (Required only in elastic case)

5. Finally, when there is no bounce, description of the system's motion reverts to equation (2-11). This time, the terminal value of Θ_L is used to initialize equation (2-12) along with $\dot{\Theta}_L'$.

6. The steps of operation continue this pattern.

14

2.4 Parameters

By referring to equations (2-12), (2-15), (2-17), and (2-24), the following parameters are available for varying:

1. $\mathcal{S}$
2. ω_n
3. θ_R
4. J_M
5. f_M
6. J_L
7. f_L
8. e

By setting ω_n equal to one, the system was made independent of its natural frequency. This normalization was discussed previously. Not shown in the preceeding list as a parameter is the gear ratio, ρ, of the gear train. Since the gear ratio was considered to have no special effect on the system, its value was set equal to one. Also not shown is the magnitude of backlash. This was not used as a parameter; however, it was assigned a value other than unity.

The motor inertia and load inertia, J_M and J_L respectively, were combined such that with ρ equal to one their sum was one. (i.e., $J_M + \rho^2 J_L = 1$) This means that any combination of J_M and J_L can be used, so long as their sum is one.

By solving equation (2-13) for the system gain constant, K, the following is obtained.

$$K = \frac{\omega_n^2 \left(J_M + \rho^2 J_L \right)}{\rho} \qquad (2\text{-}27)$$

15

Since ω_n is one, $(J_M + \rho^2 J_L)$ is one and ρ is one; the gain constant, K, must also be one. This, therefore, was the value assigned to K in this investigation.

Another variable was defined by combining the load and motor friction, f_L and f_M, similar to the way the inertias were combined. This new variable called total friction is defined as follows:

$$f_T = f_M + \rho^2 f_L \tag{2-28}$$

The friction ratio of the system is defined to be f_L/f_T.

Substituting the value of one for ω_n, ρ and $(J_M + \rho^2 J_L)$ in equation (2-14), the following results

$$2\zeta = f_M + f_L \tag{2-29}$$

or

$$\zeta = \frac{f_M + f_L}{2} \tag{2-29A}$$

Assigning a value to the damping factor, ζ, fixes the sum of $(f_M + f_L)$. To determine the value of f_M or f_L, a choice also must be made for the friction ratio. Choice of ζ and the friction ratio, therefore, fixes f_M and f_L.

For this investigation, the imput, Θ_R, was a sinusoid defined by equation (2-18). The angular frequency of oscillation, ω, was effectively normalized by making ω_n equal to one. However, the values assigned to ω were varied over the desired range of the frequency response. There is also no restriction on the choice of the forcing function amplitude A.

Equation (2-24) defines the coefficient of restitution of the gear teeth. This definition imposes no restriction on its value; practically however, it must be less than one and greater than zero.

Having so many parameters available, it was necessary to restrict their variation. Listed below are the values assigned to the various parameters. It was felt that this choice would produce the most interesting results. The method used to vary parameters will be covered in Section 3.

TABLE II-I

Values Used

for

Parameters

PARAMETER	SYMBOL	VALUES USED
Natural frequency	ω_n	1.0
Gear ratio	ρ	1.0
Backlash	Δ	.1, .05
Load inertia	J_L	.5
Motor inertia	J_M	.5
System gain constant	K	1.0
Motor friction	f_M	.12, .24, .36, .48, .60, .72, .96
Load friction	f_L	.08, .16, .24, .32, .40, .48, .64
Friction ratio	f_L/f_T	.4
Damping ratio	$\mathcal{S}$	.05, .1, .2, .3, .4, .5, .6, .8
Forcing function frequency	ω	.1 to 10.0
Forcing function amplitude	A	10, 1.0, .5, .095, .12
Coefficient of restitution	e	0, .6, .8

3. DIGITAL COMPUTER PROGRAMMING AND METHOD OF SOLUTION

3.1 Digital Computer Program

All of the frequency response results were obtained by com-
putations using the Control Data Corporation 1604 high-speed digital
computer. The computer programming was done using the Fortran system
with program input either by magnetic tape or by punched cards. Com-
puter output was put onto magnetic tape and results were printed
from the magnetic tape by use of an IBM 1401 high-speed line printer
unit.

The Fortran system was used because Fortran programming permitted
inserting the equations of the servo system into the program in forms
very close to their actual mathematical forms. The use of Fortran
also allowed a great deal of flexibility in easily modifying the program,
in changing system parameters, in inserting input data and in extract-
ing the output results in a properly labeled decimal format.

A print of a typical Fortran source program used in this inves-
tigation is shown in Appendix B. This Fortran source program, includ-
ing sub-routines, represents about 1600 machine language instructions.

The system equations to be solved by the computer were developed
in Section 2. The three differential equations describing the motion
of the combined system and the motion of the separated motor and load
were solved by subroutines which were parts of the overall Fortran
program. These sub-routines were based on the Runge-Kutta numerical
method for the solution of ordinary differential equations using a
four stage process. Each of the Runge-Kutta sub-routines utilized its

19

own integral sub-program.

Even though the system being investigated was normalized $(\omega_n = 1)$ and a unity gear ratio was chosen $(\rho = 1)$, the program was generalized to provide for changing ω_n and ρ to any desired magnitudes. Similarly, it was possible to select any value of system gain K, however a value of K = 1 was used for all calculation for reasons discussed in Section 2.

As shown in Section 2, the forcing function or input to the system in this frequency response investigation was $\theta_R = A \sin \omega t$. The amplitude A of the sinusoidal input could readily be set prior to any computer run. The sinusoidal input was obtained from the Fortran Reference Library sine function which is an integral part of the Fortran system. The input frequencies ω for each frequency response run were put into the program in an array of data. Each ω was consecutively inserted into the calculations by the program until all desired ω's were completed. A knowledge of Fortran programming is necessary to thoroughly understand how this is accomplished.

It was necessary to choose integration intervals which would yield accurate results for the Runge-Kutta solutions of the differential equations yet which would not require more calculations than necessary. It was found that for values of $\zeta \geq 0.1$ the following relationship was satisfactory for determining the intervals.

$$\text{Integration interval} \qquad \Delta t = \frac{0.001}{\omega} \qquad (3\text{-}1)$$

This resulted in 2000 x 2π solutions per input cycle for all values of input frequency ω. The values of Δt were also put into the program in an array of data and each value was inserted into the calculation along with its corresponding ω.

With combination of low ω and $\mathcal{J} < 0.1$, it was necessary to reduce Δt to a value less than obtained from equation (3-1) in order to maintain sufficient accuracy.

Since the damping ratio $\mathcal{J}$ for any run was dependent on the relative magnitudes of f_M and f_L, these parameters ($\mathcal{J}$, f_M and f_L) were set prior to each separate run and were constant for that run. All runs were made with a constant ratio of

$$\frac{\rho^2 f_L}{f_M + \rho^2 f_L} = 0.4$$

Even though the distribution of inertia between motor and load was even for all calculations, the program provided for changing this distribution to 80% of the total inertia to either the motor or load side. This was built into the program and arrays of values for J_M and J_L were put in as data similar to the arrays of ω and Δt.

The amount of backlash between the gear teeth was fixed before each computer run; in fact the value used for all but one run was $\triangle$ = 0.1 radian. A value of $\triangle$ = 0.05 was used in a special run to check the effect of changing A and $\triangle$ proportionally.

21

Because of the large number of solutions per input cycle ($\sim 000\pi$)
and since it was not necessary to record all of these results, the
program was designed to "print" the results for every one hundredth
position computation. This provided sufficient results to obtain the
frequency response of the system.

Only the steady state response, after the system transients had
effectively died out, was desired. Therefore a delay of five time con-
stants (based on a similar linear system) was included in the program so
outputs would not be 'printed' until this transient period had passed.
The program mnenomic for this was DELAY.

It was necessary to tell the program how long to compute before
switching to the next value of ω. This was done by causing the compu-
tations to shift to the next ω when a predetermined amount of problem
time had elapsed after the transient period. This time was based on a
desired number of input cycles. The program mnemonic for this was
designated CYC.

3.2 Sequence of Solution of System Equations

The starting condition for each frequency response run was with
the gear teeth in contact, i.e. the motor and load were combined, with
this equation describing the system motion:

$$\ddot{\theta}_c + 2\mathcal{S}\omega_n \dot{\theta}_c + \omega_n^2 \theta_c = \omega_n^2 A \sin \omega t \qquad (3\text{-}2)$$

This differential equation was solved as each increment of sinusoidal
input was added. The corresponding value of θ_c was calculated and the

22

combined phase plane slope was computed by

$$N_c = \frac{\ddot{\Theta}_c}{\dot{\Theta}_c} \qquad (3\text{-}3)$$

This slope was compared with the computed value of the load-alone slope, which was constant for the run;

$$N_L = -\frac{f_L}{J_L} \qquad (3\text{-}4)$$

When $N_C = N_L$ the motor and the load were commencing to separate. If the system velocity $\dot{\Theta}_c$ was positive at separation the gear teeth were separating from the original contact position.

If $\dot{\Theta}_c$ was negative, the teeth were separating from the opposite side of the backlash.

After separation, the equation describing the motor motion was

$$\ddot{\Theta}_M + \frac{f_M}{J_M} \dot{\Theta}_M + \frac{K}{J_M} \Theta_L = \frac{K}{J_M} A \sin \omega t \qquad (3\text{-}5)$$

This differential equation was solved for each input increment. At the same problem time t, the following differential equation for the load alone was solved:

$$\ddot{\Theta}_L + \frac{f_L}{J_L} \dot{\Theta}_L = 0 \qquad (3\text{-}6)$$

From these solutions, the positions of the motor and load were compared in order to determine when the gear teeth had re-touched on

23

either side of the backlash. A condition to be satisfied for re-touching was

$$\theta_L = \rho\, \theta_M \qquad\qquad (3\text{-}7)$$

or

$$\theta_L = \rho\, \theta + \Delta \qquad\qquad (3\text{-}8)$$

When the teeth did make contact, the load velocity after touching was calculated from

$$\dot{\theta}_L' = \frac{J_M}{J_M + \rho^2 J_L}\left[\rho\,\dot{\theta}_M\,(1+e) + \dot{\theta}_L\left(\frac{\rho^2 J_L}{J_M} - e\right)\right] \qquad\qquad (3\text{-}9)$$

and the motor was

$$\dot{\theta}_M' = \frac{\dot{\theta}_L' - e\left(\rho\,\dot{\theta}_M - \dot{\theta}_L\right)}{\rho} \qquad\qquad (3\text{-}10)$$

The following equation was then solved to see if the teeth stayed combined

$$\text{Is}\quad \rho\,\dot{\theta}_M - \dot{\theta}_L \leq \epsilon \ ? \qquad\qquad (3\text{-}11)$$

Where ϵ was an arbitrarily small number which was used to determine when the velocities were almost equal in the case of elastic impact.

When the teeth stayed combined, the program returned to the combined differential equation (3-2) and the complete sequence was repeated.

24

3.3 Printing of Results .

Solution of any of the three differential equations of the system produced the values of the respective position Θ and velocity $\dot{\Theta}$. Since the position and velocity of the combined system were defined as the load or output position and velocity, these values of Θ_c and $\dot{\Theta}_c$ were printed as the outputs when the gear teeth were in contact. When the motor and load were separated, the load alone was printed as the output, and the motor position and velocity were also printed for the same problem time t.

For each print of system position and velocity, the problem time and the input position were also printed. Prints were made for each one hundredth solution of the differential equation or equations concerned. Special prints of problem time, position(s), velocity(s) and input were made just after the gear teeth separated or combined. A typical print of computer output is shown in Appendix C. This shows that output position and velocity $(\Theta_c$ and $\dot{\Theta}_c)$ only were printed when the system was combined, while motor and load positions and velocities also were printed when the teeth were separated.

Only five decimal places of results were printed because of limitations in the accuracy of plotting results. The computational accuracy was somewhat greater since the Runge-Rutta method was accurate to about $(\Delta t)^5$, which was 10^{-10} for the largest Δt used.

A complete computer program flow chart and explanation is included in Appendix A.

3.4 Computation Time

Computer operating time to obtain a steady state output varied
considerably for different values of $\mathcal{S}$ and for the different input
frequencies ω. For example, to compute through a five time constant
transient period, with a low damping ratio of $\mathcal{S} = 0.1$ (long time con-
stant) and with an ω of 2.0 (small integration interval), required
about 28 minutes of computation. On top of this, it took about one
and three-quarter minutes to compute and print the outputs for each
input cycle. From one to eight cycles of input (after the estimated
transient period) were required to obtain a steady state peak output.
For the other extreme of a high $\mathcal{S}$ of 0.8 and a low ω of 0.1, the
total computation and print time required to obtain an output peak
took only about two minutes.

It is apparent that the investigation required a great amount
of computer time. All computer runs, including test runs, took a
total of about 83 hours of computer operation.

An attempt was made to develop a computer program which would
approximate the energy stored in the system for steady state at the
first input frequency and would retain this "stored energy" when ω
was changed. It was hoped this would materially reduce the transient
period in reaching steady state at the new ω. Test runs were promising
but time did not permit refinement of this program to where it could
be used in the investigation.

4. RESULTS AND DISCUSSION

4.1 Determining M from the Computer Output

From standard frequency response nomenclature, the symbol M is defined to be the magnitude of the ratio of system output to system input. Symbolically this is:

$$M = \left| \frac{\theta_c}{\theta_R} \right| \tag{4.1}$$

where

$$\left| \theta_R \right| = A$$

Appendix C shows a sample print out of data from the computer. One of the quantities printed is output position. To determine $\left| \theta_c \right|$, it was necessary to pick off the value of output position at its maximum or minimum. In general, there were two peaks. One was a positive peak and the other a negative peak. These two peaks came about because the input was permitted to go through only one cycle once printing began. The magnitude of these peaks were not always identical. This indicated that the system had not reached steady state; however, in most cases, the difference between the peaks was less than plotting accuracy. The average of the magnitude of these peaks was taken to be $\left| \theta_c \right|$.

With values of the damping ratio greater than about .4, the method of obtaining $\left| \theta_c \right|$ as described above was used. At damping ratios of about 0.3 and lower, there began to appear an oscillation at the natural frequency of the system super-imposed on the output wave form. Its

27

presence could be expected when a limit cycle would be predicted by Ref. (2).

Fig. 4-1a shows this phenomenon. The damping ratio, $\mathcal{J}$, was 0.1 in this case. Shown in Fig. 4-1b is the output waveform of the same system with a higher damping ratio. ($\mathcal{J} = 0.5$) It can be seen here that there is no super-imposed "limit cycle". To obtain $|\theta_c|$ for the system whose output is shown in Fig. 4-1a, it was necessary to take the mean of the super-imposed oscillation. In the case shown, this was not particularly difficult. However, as ω was increased towards the undamped natural frequency, this procedure became more difficult. Fig. 4-2a shows the output waveform for the same system at $\omega = .6$. From this figure, it can be seen that it is virtually impossible to establish the mean of the "limit cycle" oscillations. Even if the output wave shape were available for a longer time period, it would still be virtually impossible to obtain an accurate mean value. To compare the output at the same forcing frequency, but with higher damping ratio, Fig. 4-2b was drawn. Here $\mathcal{J} = 0.5$, and it can be seen that there is no difficulty picking the peak output value.

Since the method of picking $|\theta_c|$ varied, it was not possible to program the selection of $|\theta_c|$. In some cases, a programmed method would have been satisfactory, but unless all the data were examined, the value of $|\theta_c|$ thus obtained would be questionable.

4.2   Frequency Response Variation with Damping Ratio

Frequency response curves, for plastic impact of the gear teeth, were obtained for values of $\frac{A}{\Delta}$ of 10, 5 and 0.95, with damping ratio $\mathcal{Y}$ varying from 0.1 to 0.8. These curves are shown in Figures 4-3, 4-4 and 4-5 respectively. For comparison purposes, a similar family of curves for a comparable linear system is shown in Fig. 4-6.

It was determined by test runs, where both A and Δ were varied proportionally, that the frequency response was identical as long as the ratio $\frac{A}{\Delta}$ was constant. For example, the same frequency response resulted with A = 1.0 and Δ = 0.1 as with A = 2.0 and Δ = 0.2. This makes the frequency response results generally applicable to all simple second order servo systems for the same relative amounts of backlash since the system was normalized with ω_n = 1. For this reason the abscissae of the curves are labeled ω/ω_n, and the curves can be applied to any simple second order system by multiplying by ω_n of the system.

The resonant frequencies, for values of damping ratio that resulted in resonance ($\mathcal{Y} \leq 0.6$), were found to increase as the amount of backlash was increased. This increase in resonant frequency was greatest for the higher values of $\mathcal{Y}$ while it was almost insignificant at a $\mathcal{Y}$ of 0.1.

The peak values of the ratio of output position to input amplitude at resonance M_p, increased above the linear peaks as the amount of backlash was increased. The increase was greatest at the lowest value of $\mathcal{Y}$. A plot showing this variation from the linear for different amounts of backlash is shown in Fig. 4-7.

As might be expected, the effect of backlash is greatest at the resonance frequencies. The frequency response curves, for all amounts of backlash, are above the linear curve at values of ω below the resonant frequencies. At frequencies greater than the undamped natural frequency and for values of $\mathcal{Y} > 0.4$, the response with backlash drops off more rapidly than the linear and the degree of drop-off is greater as the backlash is increased. In the same frequency range, the response curve at low values of $\mathcal{Y}$ is slightly above the linear curve (ignoring sub-harmonic resonance which will be discussed later). This indicates that with heavy damping, backlash results in a more rapid attenuation of output at frequencies above the undamped natural frequency of the system, while with light damping, attenuation is slightly less than the linear up to $2\,\omega_n$.

4.3   Effect of Magnitude of Backlash on Frequency Response for Constant $\mathcal{Y}$.

A more detailed examination of the effect of the amount of backlash in the system compared with the input amplitude was made for a constant damping ratio. The value of $\mathcal{Y} = 0.5$ was chosen since it represents a practical damping ratio which is less than optimum and results in a moderately oscillatory system. Also, no limit cycle exists at this value of $\mathcal{Y}$ according to Anderson and Luckett, Ref. 2. It was pointed out earlier that as long as the ratio of A/Δ is constant the frequency response is invariant. Therefore, A/Δ is a logical system parameter.

Figure 4-8 shows the frequency responses at $\mathcal{Y} = 0.5$ for A/Δ of 10, 5 and 0.95 with plastic impact of the gear teeth. The linear response is also shown on the plot. It can be seen that the response deviated from the linear even when the magnitude of backlash was only one-tenth of the input amplitude. The deviation increased as the relative magnitude of backlash was increased. The effect of backlash was to change the response curve to resemble the response for a lower damping ratio.

At frequencies above the undamped natural frequency, with $A/\Delta = 0.95$, the response curve dropped below the linear curve and reached a minimum near $\omega = 2$. Up to this input frequency the ratio of output frequency to input frequency was one to one. With a slightly higher ω, the ratio of output to input frequencies f_o/f_i rapidly transitioned to 1/2 and the magnitude of the output abruptly increased. This was the first of a series of sub-harmonic resonance peaks which were encountered as ω was increased further. The actual values of M

31

between sub-harmonic resonance peaks were not all definitive as will be shown in the discussion of the output wave shapes for this region of ω. At some frequencies where input frequency was not an integer multiple of the output frequency, the output magnitude could not be defined because of the random, unsteady nature of the load position. This is shown by a dashed line in Fig. 4-8.

4.4 Sub-harmonic Resonance with Plastic Impact

The first sub-harmonic resonance peak occurred at $\omega = 2.2$, (Fig. 4-8). At input frequencies of 2.0 and below, the outputs were steady with amplitudes decreasing with increasing ω, and the ratios of output to input frequencies were $1/1$. The wave shapes of the output for $\omega = 1.8$, 1.9 and 2.0 are shown in Figs. 4-9 and 4-10. At $\omega = 2.1$ the output was very unsteady (Fig. 4-10b) and a value for M could not be determined. At this input frequency, the ratio of output frequency to input frequency f_o/f_i was not constant but fluctuated with an average of between $1/1$ and $1/2$.

When ω was increased to 2.2, the frequency ratio f_o/f_i became a steady $1/2$. The output wave shape became steady but unsymmetrical, as shown in Fig. 4-11a. The peaks of this output wave occurred at the times of contact of the gear teeth. The reason for the unsymmetrical wave shape was due to the difference in relative velocities of the motor and load at the time of contact. Referring to Fig. 4-11a, the higher (positive) peaks occurred as a result of the lower relative velocity at the instant prior to the preceding contact (smaller peaks). This smaller relative velocity imparted a higher velocity to the load which

32

caused a greater excursion. The opposite was true in going from contact at the higher peaks (high relative velocity) to the smaller peaks. This phenomenon is believed to be related to the fact that there was plastic impact of the gear teeth. The value of M at the sub-harmonic resonant peak at $\omega = 2.2$ in Fig. 4-8 came from the average of the high and low peaks.

When ω was increased to 2.3 the output wave became erratic, the ratio f_o/f_i was transitioning from 1/2 to 1/3 and the exact value of M was indeterminant but was obviously less than at $\omega = 2.2$ (Fig. 4-11b).

At $\omega = 2.4$ the output wave (Fig. 4-12a) was similar to the wave shape at the previous sub-harmonic resonance peak of $\omega = 2.2$. The wave was steady but unsymmetrical and the ratio of f_o/f_i was a fixed 1/3. The value of M was further reduced (averaged from peaks of output wave).

Going to $\omega = 2.5$ (Fig. 4-12b) the wave shape was again unsteady but f_o/f_i was a consistent 1/3 and M began to increase. This increase in M continued for the next four ω's.

Wave shapes for ω's 2.6, 2.7, 2.8 and 2.9 shown in Figs. 4-13 and 4-14, show very convincingly a sub-harmonic resonance. At $\omega = 2.6$, the general wave shape of the output during this resonance is first observed. For all four of these frequencies, the system output had the same wave shape. As the frequency was increased, the M value also increased. All four of these frequencies gave a f_o/f_i of 1/3. Just as the output wave shape was very steady, the f_o/f_i was equally as steady at 1/3. The sub-harmonic rise associated with these frequencies is shown on Fig. 4-8. Since the value of M for these frequencies was so well defined, this portion of the curve was not dashed as was required for

frequencies between $\omega = 2.0$ and $\omega = 2.4$.

A further increase in frequency beyond $\omega = 2.9$ resulted in a drop-off in M. Fig. 4-15 shows the output wave shape for $\omega = 3.0$. This wave shape was taken for a period of over 50 time constants. As can be seen, there are portions of this wave which are quite steady and portions which are very unsteady. The steady portion had a f_o/f_i of 1/3. The M value taken from this steady portion was used to plot on Fig. 4-8. No M value could be obtained from the unsteady portion due to its inconsistent movement. The f_o/f_i during the unsteady portions was not defined either. It averaged between 1/3 to 1/4.

At frequencies greater than 3.0, the output motion was erratic. This can be seen in Fig. 4-16 for $\omega = 3.1$ and 4.0 as well as in Fig. 4-17 for $\omega = 5.0$. Since M could not be deduced from these wave shapes, no points are plotted on Fig. 4-8 beyond $\omega = 3.0$.

The f_o/f_i for $\omega = 3.1$, Fig. 4-16a, was 1/3. This may be misleading because only a small amount of the output wave was obtained. At $\omega = 4.0$, Fig. 4-16b, the f_o/f_i was between 1/4 and 1/5. Fig. 4-17, for $\omega = 5.0$, shows the output wave shape for a considerable time. It can be seen here that the wave was not consistent. The f_o/f_i for this ω varied widely. Depending on the portion of the curve examined, the f_o/f_i was as small as 1/6 and as large as 1/4.

Although no sub-harmonic resonance was found beyond $\omega = 2.9$, it would appear that it does exist. In transitioning from one sub-harmonic frequency to another, the output wave was quite unsteady. When a definite output frequency was established, the M was also defined. Since the f_o/f_i ratio changed from 1/3 at $\omega = 2.9$ to 1/6 at

34

$\omega = 5.0$, a sub-harmonic resonance at $1/4$ and $1/5$ must have occurred between these two frequencies.

From the limited data available, it appears that the system tends to resonate at odd sub-harmonics. Frequencies between $\omega = 2.0$ and $\omega = 2.2$ did not have a fixed f_o/f_i. Then at $\omega = 2.2$, a steady $1/2$ ratio was observed.

During the build up to the third sub-harmonic resonance peak, a steady ratio of $1/3$ was present. This steady f_o/f_i over several values of frequency, leads one to believe the system would tend to seek an odd sub-harmonic frequency. Immediately past the sub-harmonic peaks, the system began seeking the next sub-harmonic frequency. The even sub-harmonics did not appear steady except at $\omega = 2.2$. There was a considerable range, $\omega = 2.4$ to $\omega = 2.9$, where f_o/f_i was a steady $1/3$ adding support to the belief that the system would seek odd sub-harmonics.

4.5   Effect of Elastic Impact

Frequency response data were obtained, at a constant $\gamma = 0.5$, for
values of A/Δ equal to 10, 5 and 0.95 with $e = 0.6$ and $e = 0.8$. These
parameters were the same as for the results discussed in Section 4.3,
except for the values of the coefficient of restitution e. The response
curves for $e = 0.6$ and $e = 0.8$ are shown in Figs. 4-18 and 4-19. The
values of M for all three values of A/Δ were found to be slightly
less for both cases of elastic impact than for $e = 0$ (Fig. 4-8) at
frequencies near resonance. This indicates that elastic impact tends
to reduce M_p as compared with plastic impact. There was practically no
difference between the response curves for $e = 0.6$ and $e = 0.8$ up to
input frequencies of $\omega = 2$.

With $A/\Delta = 0.95$ sub-harmonic resonance began to occur at about
$\omega = 2.8$ for $e = 0.6$. Up to $\omega = 2.7$ (Fig. 4-20a) the ratio f_o/f_i was
a steady 1/1 and the output wave shapes were steady and symmetrical.
At $\omega = 2.8$ the output waveshape became erratic (Fig. 4-21a) and f_o/f_i
was transitioning from 1/1 to 1/2. The response curve remained above
the linear at all frequencies (Fig. 4-18), unlike the equivalent curve
for $e = 0$ (Fig. 4-8) which dropped below the linear between M_p and the
occurrence of sub-harmonic resonance.

The response curve reached a minimum at $\omega = 2.8$. At the next
test frequency $\omega = 2.9$, the output increased and the ratio f_o/f_i was
between 1/2 and 1/3. No even harmonic was found as there was for $e = 0$.
The wave shape at $\omega = 2.9$ was also uneven with very inconsistent peaks
(Fig. 4-20b). At $\omega = 3.0$ and $\omega = 3.2$, f_o/f_i was still between 1/2 and

36

1/3 the value of M was increasing with unsteady waveshapes (Figs. 4-21b and 4-22a). At $\omega = 3.4$ (Fig. 4-22b) f_o/f_i became a consistent 1/3 and M remained about the same, but the wave shape was still not steady. As ω was increased to 3.7 and to 4.0 (Fig. 4-23) the waves became symmetrical, f_o/f_i remained 1/3 and the value of M was decreasing. At the highest test frequency $\omega = 4.3$, M was still decreasing, the wave shape was becoming unsymmetrical (Fig. 4-24) and f_o/f_i was decreasing toward 1/4.

In comparing the response curves of Fig. 4-8 ($e = 0$ and Fig. 4-18 ($e = 0.6$) for $A/\Delta = 0.95$, it can be seen that the addition of bounce changed the curve and the sub-harmonic resonance pattern at frequencies above ω_n. Bounce eliminated the drop of the response curve below the linear response and apparently also eliminated the even sub-harmonic resonance peak. The odd (1/3) sub-harmonic resonance peak was lower with bounce but was wider, i.e. the value of $f_o/f_i = 1/3$ persisted over a wider range of frequencies. Sub-harmonic resonance started at a higher frequency when bounce was introduced.

For $e = 0.8$ and $A/\Delta = 0.95$, sub-harmonic resonance started to occur at about the same value of ω as for $e = 0.6$. The investigation did not go beyond this frequency for $e = 0.8$.

In general, elastic impact of the gear teeth tended to reduce the effects of the nonlinearity for both the magnitude of the output and the amount of sub-harmonic resonance.

4.6 Response Characteristics with Very Low Damping Ratio

In an effort to find jump resonance and the factors influencing its occurrence, some runs were made with a damping ratio, $\mathcal{Y}$, equal to

0.05. Considerable computer time was required for calculating the output at such a low damping ratio. Therefore, only a limited number of frequencies were investigated.

The basic parameters for this investigation were: damping ratio equal to 0.05, A/Δ equal to 1.2, coefficient of restitution equal to zero. The frequencies used were between 0.5 and 1.8 with emphasis on the frequencies near the undamped natural frequency. Results of these runs did not show any jump resonance; however, some interesting things were shown.

For a linear system, the resonant frequency is always less than the undamped natural frequency. (Resonant frequency is the frequency at which the resonant peak occurs on a frequency response.) Regardless of how small the damping ratio gets, the resonant frequency is always less than the undamped natural frequency; however, as $\mathcal{Y}$ approaches zero the resonant frequency approaches but never exceeds the undamped natural frequency.

With backlash present, this is not always so. Fig. 4-25 shows a resonant peak at a frequency between 1.01 and 1.02 which was greater than ω_n. It has been shown previously that the effect of increasing backlash was similar to reducing the damping ratio. In addition to this effect, it appears that with a sufficiently large backlash and small enough $\mathcal{Y}$, the resonant frequency is increased more than the increase associated with a reduction in $\mathcal{Y}$ alone. This may not be limited to low damping ratios. It may have occurred at higher damping ratios but was masked due to insufficient data being taken in the vicinity of the resonant peak.

38

The height of the resonant peak for this low $\mathcal{Y}$ is considerably higher than for the linear case. However, extrapolation of Fig. 4-7 gives approximately the same value for this peak as shown on Fig. 4-25. At frequencies near the resonant frequency, between 0.95 and 1.05, the output wave shapes were steady. The frequency ratio was also steady at one to one. Fig. 4-26 shows the output wave shape at $\omega = 0.95$ and Fig. 4-27 shows it at $\omega = 1.0$. As ·can be seen, these are steady.

The output below $\omega = 0.9$ was rather difficult to interpret. By the previously discussed methods for obtaining M, it was not possible to determine this quantity accurately. Therefore, values of M for these frequencies were not plotted on Fig. 4-25.

Fig. 4-28 shows the wave shape for $\omega = 1.2$. Even though the output wave shape is steady at this frequency, the input frequency is not an even multiple of the output frequency. This uneven relationship has been mentioned previously (Section 4.4) as an indication of the onset of sub-harmonic resonance. Therefore, the low damping ratio decreases the frequency at which sub-harmonic resonance appears. Insufficient data are available to determine the exact location of the first sub-harmonic resonant peak, but it appears to occur at a frequency near $\omega = 1.6$. The M at this peak is approximately 9, and the frequency ratio is even at one to two.

4.7   Test of Program and Validity of Results

For there to be complete confidence in the results of this investigation, some mention should be made of the steps taken to prove the computer program from which the results were obtained. Also, some mention of the validity of the results is in order. It is the purpose of this section to discuss these subjects.

Since there was no easy way that the system investigated could be simulated on an analog computer; and since little information is available on such non-linear systems, it was necessary to test the program by approximation. First of all, the program was divided into two basic parts. These were, the combined system portion and the separated system portion. As integral parts of these two sections were the basic decisions which had to be made to transfer from one to the other.

It was rather simple to test the combined section. This was done by setting the backlash, Δ , equal to zero. Doing this effectively eliminated the separated system portion and the decisions required to transfer into that portion. With the backlash equal to zero, the output should be the same as the output from a linear system. Comparison of the M obtained from the print out data, as described in section 4-1, with linear results obtained by conventional means were very favorable. The slight differences could be attributed to the computer solution still being in a transient state. The data from the computer solution was taken after five time constants had elapsed. The following table shows this comparison.

TABLE IV-1

$\mathcal{Y} = .8$ $\Delta = 0$

ω	M, computer	M, linear
.1	.99714	.99716
.2	.98810	.98821
.3	.97172	.97197
.4	.94693	.94694
.5	.91180	.91192

It was not possible to test the separated portion alone. There-
fore, it was necessary to test this portion as part of the overall test
of the program. For a linear system, the ratio of forcing function am-
plitude to the amount of backlash, A/Δ , is infinite since the backlash
is zero. Therefore, if this infinite ratio is approximated by a non-
linear system, the results should be very close to linear results. To
approximate the linear system, an A/Δ of 100 was chosen. The results
of this test run were within 2.5 percent of the linear response at all
frequencies less than the resonance frequency. At frequencies above
resonance, the non-linear response was less than five percent different
than the linear response out to the highest frequency used. The maximum
percent difference occurred at the highest frequencies where small dif-
ferences account for higher percentages.

Since the program was capable of approximating a linear system
while actually going through all of the calculations necessary for a non-
linear system; it was reasonable to assume that with a greater amount

of backlash, smaller $\frac{A}{\Delta}$, the program would give valid results.

Even though the time solution of the differential equations was considered accurate, the method of determining M may have introduced inaccuracies. For damping ratios greater than 0.3, the method of obtaining M was quite accurate. The only improvement would have been to calculate for a longer time, but this would have required more time than could be justified by the increased accuracy.

At damping ratios less than 0.3, the interpretation of the output waveform, Θ_c, was not so clear cut. At these damping ratios, the "limit cycle" was super-imposed on the output wave. At some frequencies, ω less than about 0.4, the method used to obtain M was quite good. (Mean of "limit cycle" oscillations) However, for frequencies between about 0.4 and 0.7, the M was not so nicely defined. It was in this frequency range for low $\gamma's$ that the results were not as accurate as they were otherwise. At all frequencies above an ω of about 0.7, the results were quite good except as dicussed in the sub-harmonic section.

Mention has been made that data was taken after five time constants based on a linear system. The wave shapes at earlier times were looked at to determine if this delay were required. From these, it was evident that the system was in a transient state. Even after five time constants, there was evidence of transients. However, the transient affect was quite small. Depending upon the parameters, the transient was virtually gone shortly after five time constants had elapsed. The only exception to this was discussed as part of sub-harmonic resonance. In the cases where steady state was reached, it was reached in less than six time constants.

4.8 Application of Results and Extension of Method

While there is limited direct application of the results of this investigation to servo design, there are some points that could prove helpful in the design of certain types of systems. If a system with backlash were to be operated with a periodic input, Fig. 4-7 would be useful in determining how much backlash could be tolerated for a given input amplitude to meet specified peak outputs. Also, the results showing the effect of gear resilience can be of benefit in choosing a gear material, since higher resilience tends to reduce the effect of the backlash.

The general form of the computer program can be adapted to calculate any particular frequency response of similar second order systems with known system constants (K, J_M, J_L, Δ, etc.) for specified parameters. The program can be very easily modified to obtain transient response of second order systems with any desired sets of constants and parameters. Similarly, it can be readily applied to steady state (limit cycle) investigations.

As has been pointed out, the method of obtaining frequency response results in this investigation requires a great deal of digital computer time. If further investigations were to be based on the same general approach, especially at very low damping ratios, a technique of going from one frequency to another without having to go through a new transient period each time, should be devised. Such a program was briefly attempted, as mentioned in Section 3, which transferred boundary conditions of the differential equations at the first frequency to the

43

appropriate differential equations as initial conditions at the next frequency. This was an attempt to utilize the "energy" stored in the system to more rapidly set up a steady state condition for the next frequency. It appears this concept may be the only way that would make feasible this digital method to more extensive investigations. It could result in showing jump resonance when it exists, where the program used herein apparently did not.
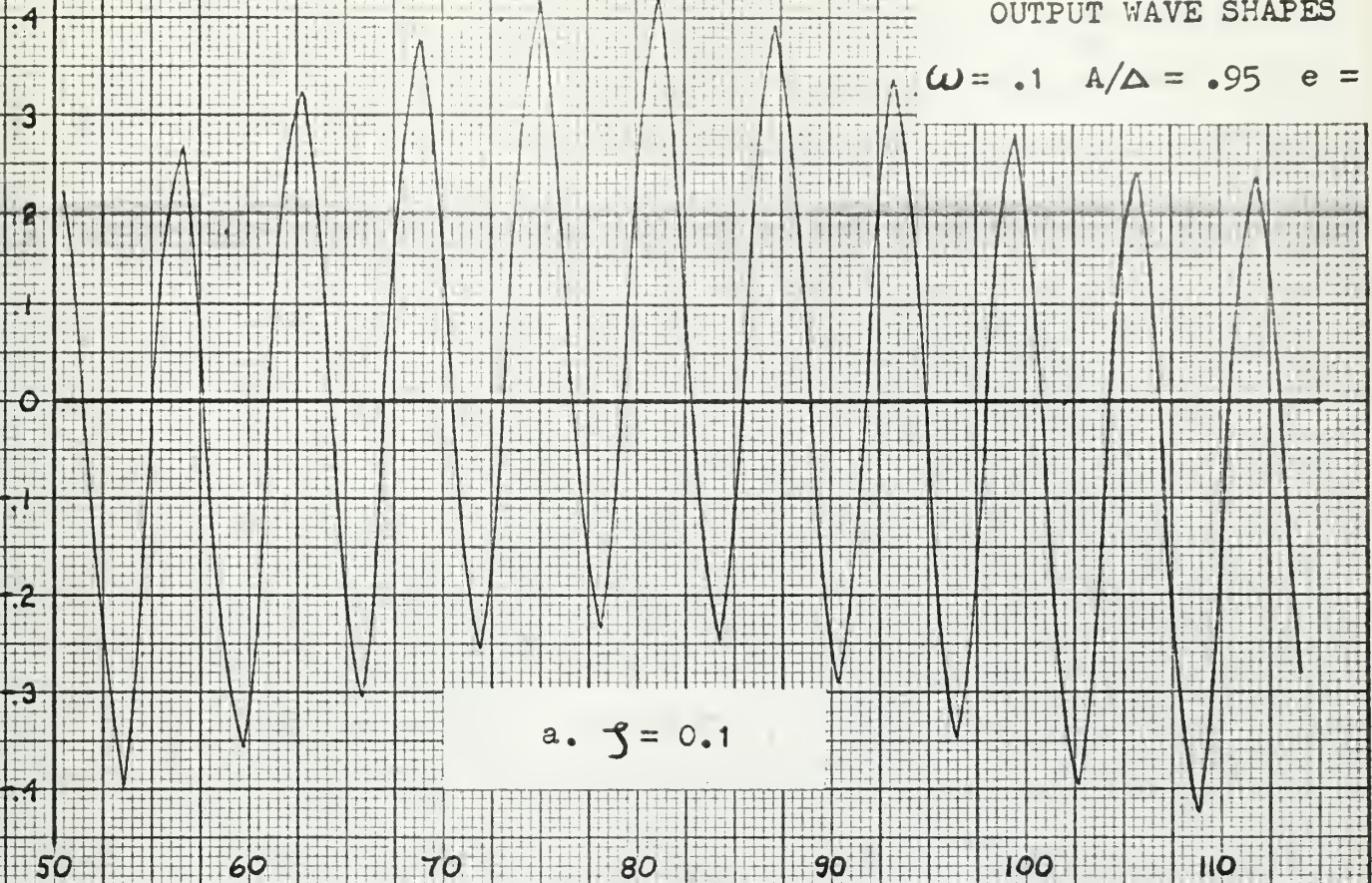
Fig. 4-1

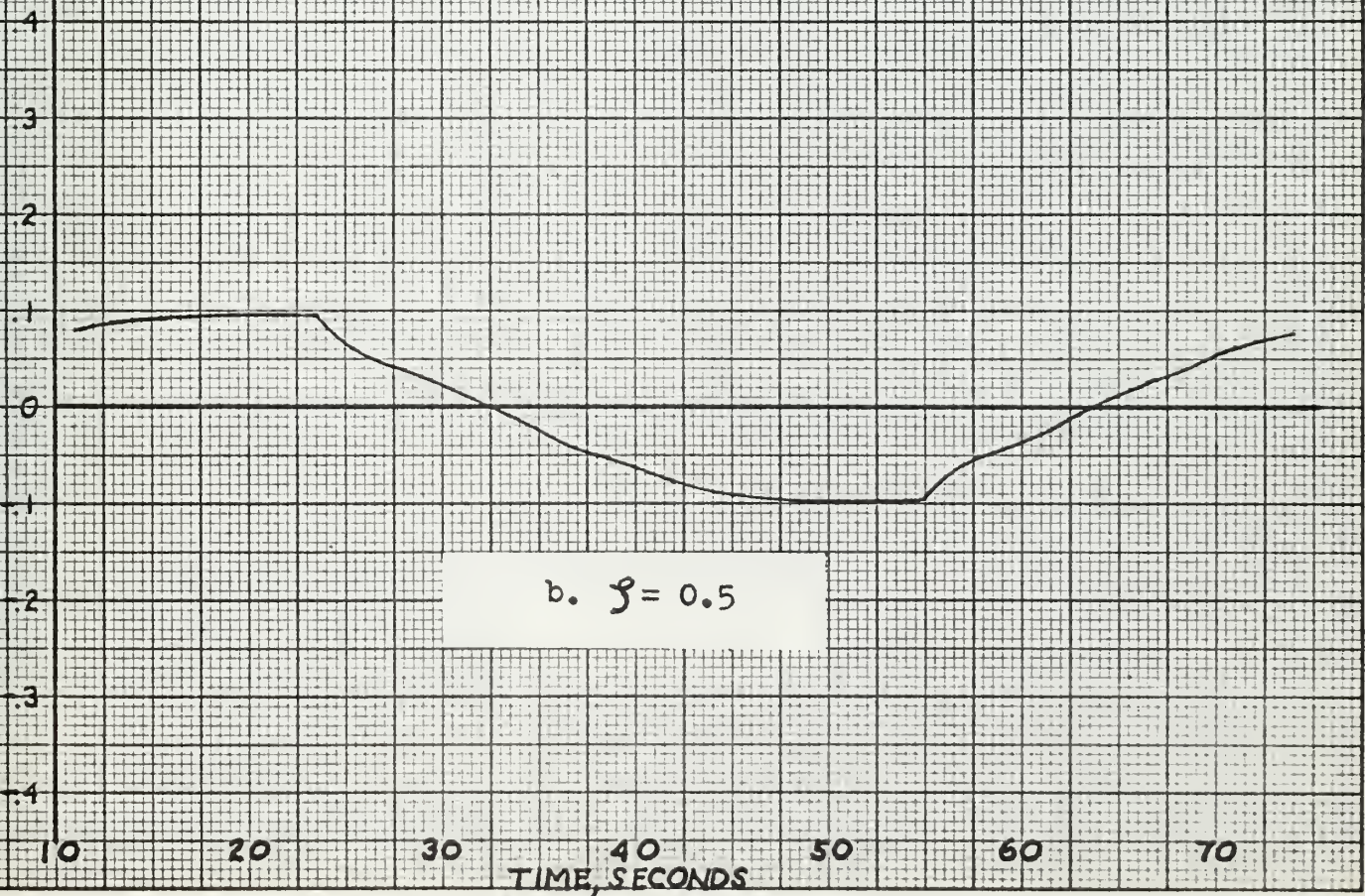OUTPUT WAVE SHAPES

$\omega = .1 \quad A/\Delta = .95 \quad e = ($

a. $\zeta = 0.1$

TIME, SECONDS

b. $\zeta = 0.5$

TIME, SECONDS

45

Fig. 4-2

OUTPUT WAVE SHAPES

$\omega = .6$ $A/\Delta = .95$ $e = 0$

a. $\mathcal{S} = .1$

b. $\mathcal{S} = .5$

OUTPUT POSITION, θ_c, RADIANS

TIME, SECONDS

OUTPUT POSITION, θ_c, RADIANS

TIME, SECONDS

46

Fig. 4-3

FREQUENCY RESPONSE WITH PLASTIC IMPACT
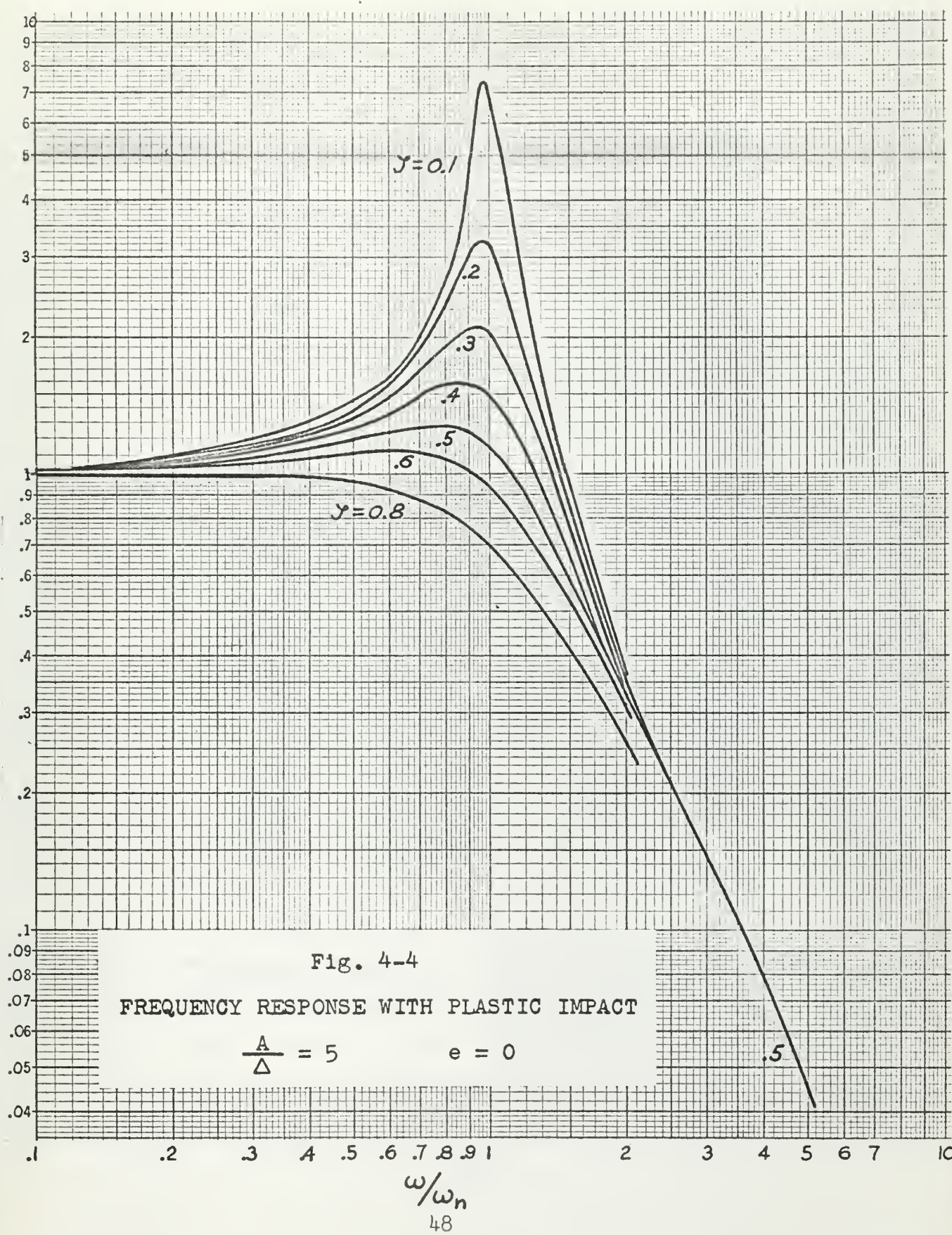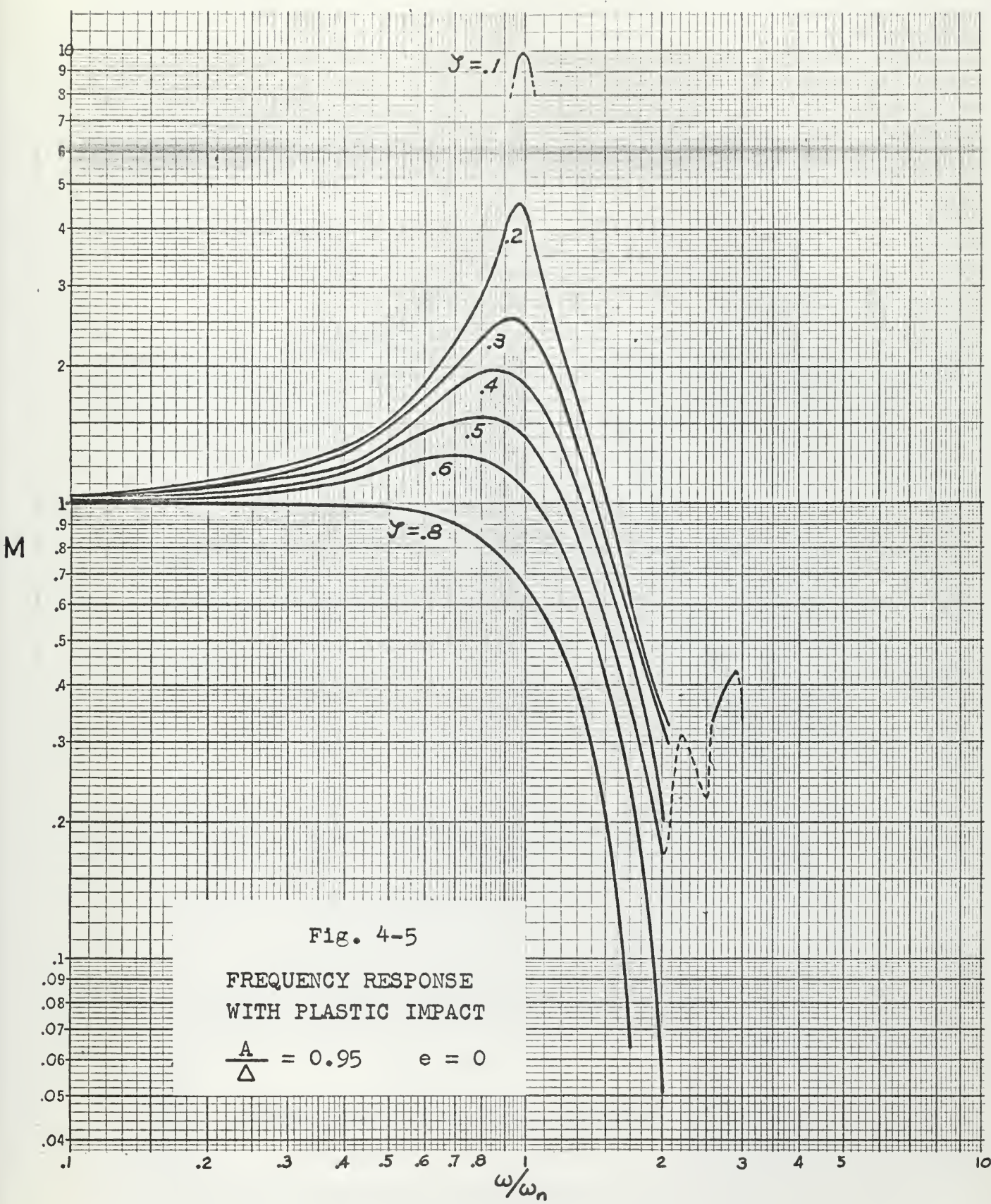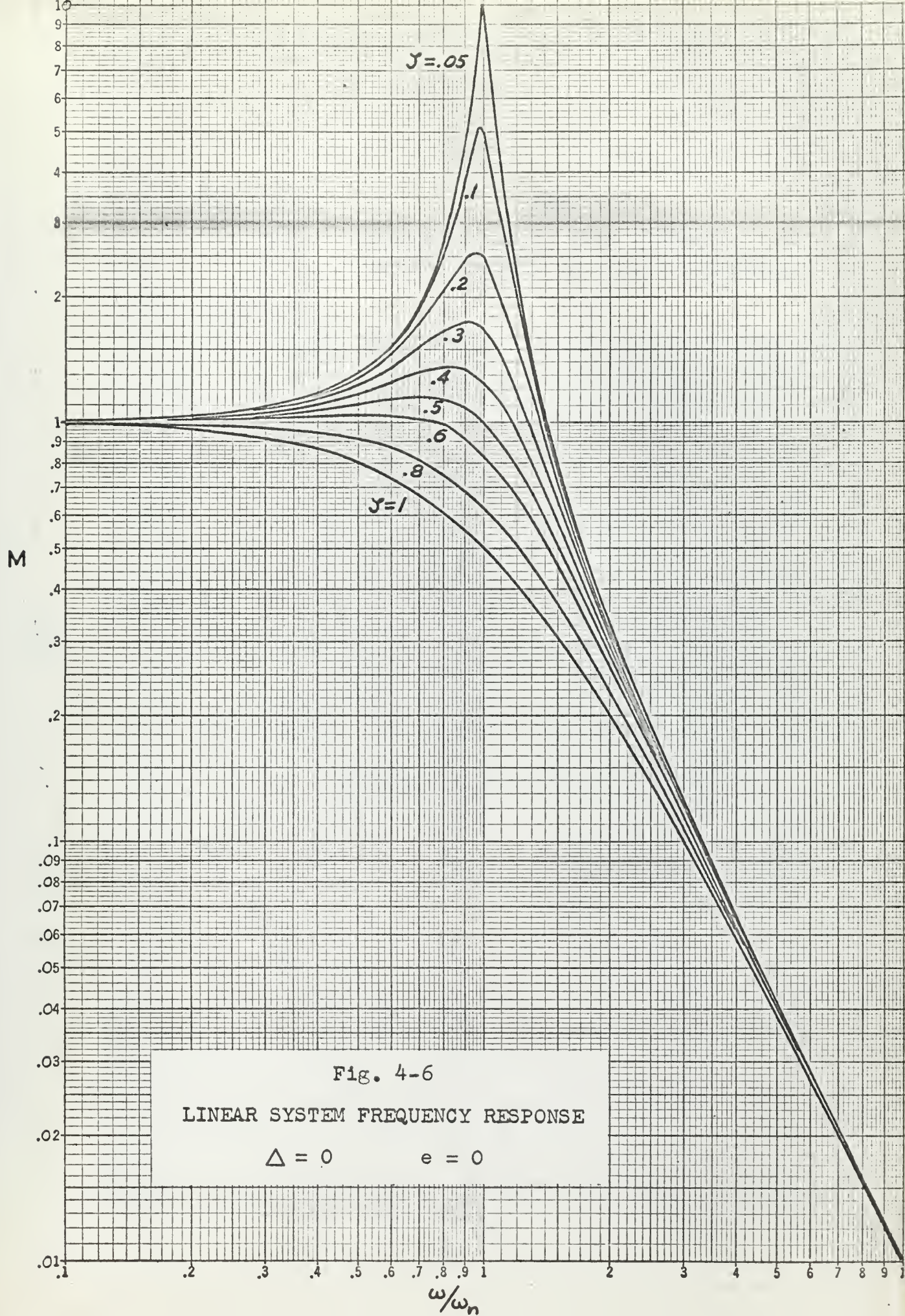
$$\frac{A}{\Delta} = 10 \qquad e = 0$$

47
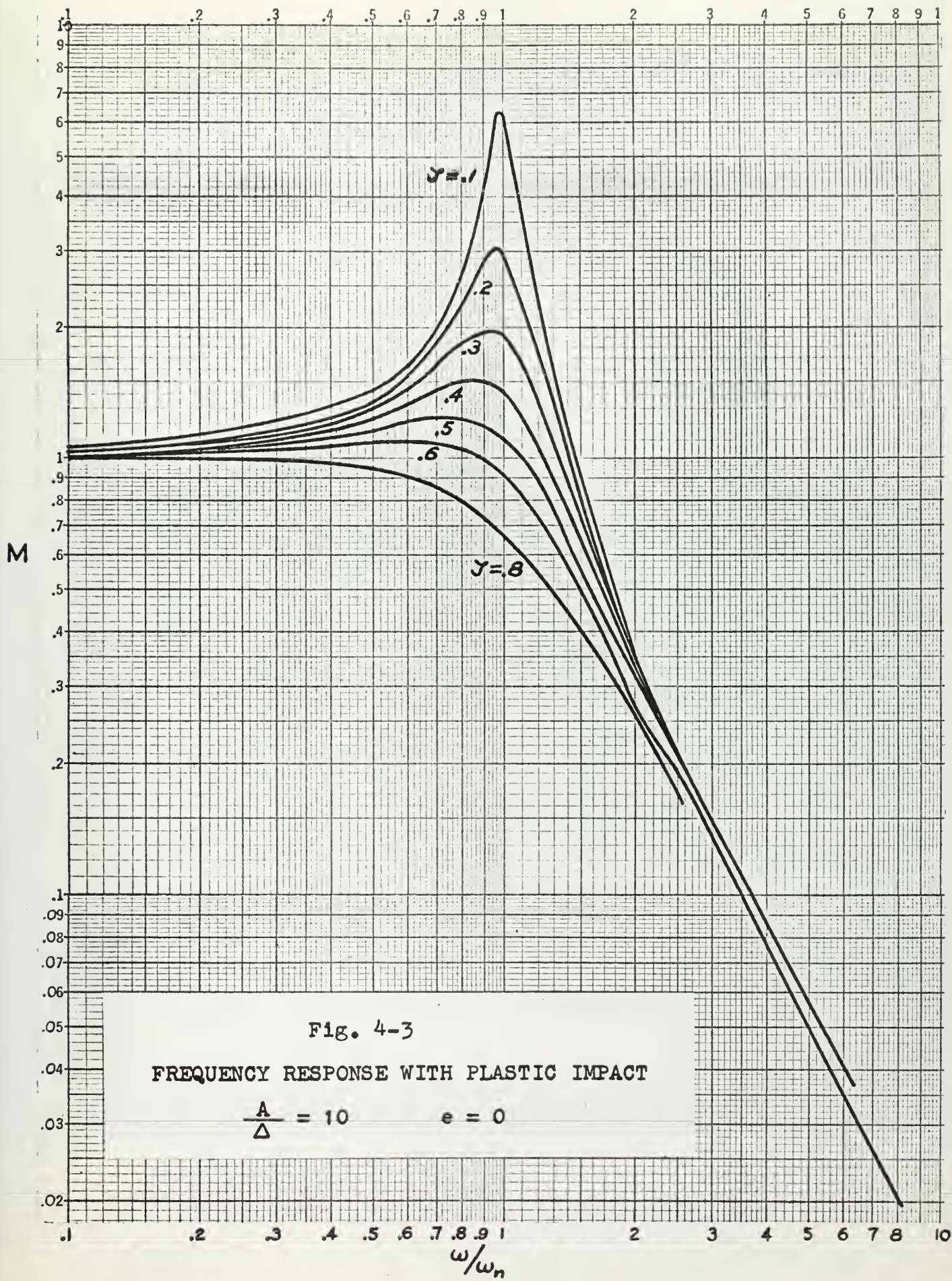
Fig. 4-4

FREQUENCY RESPONSE WITH PLASTIC IMPACT

$\frac{A}{\Delta} = 5 \qquad e = 0$

48

Fig. 4-5

FREQUENCY RESPONSE
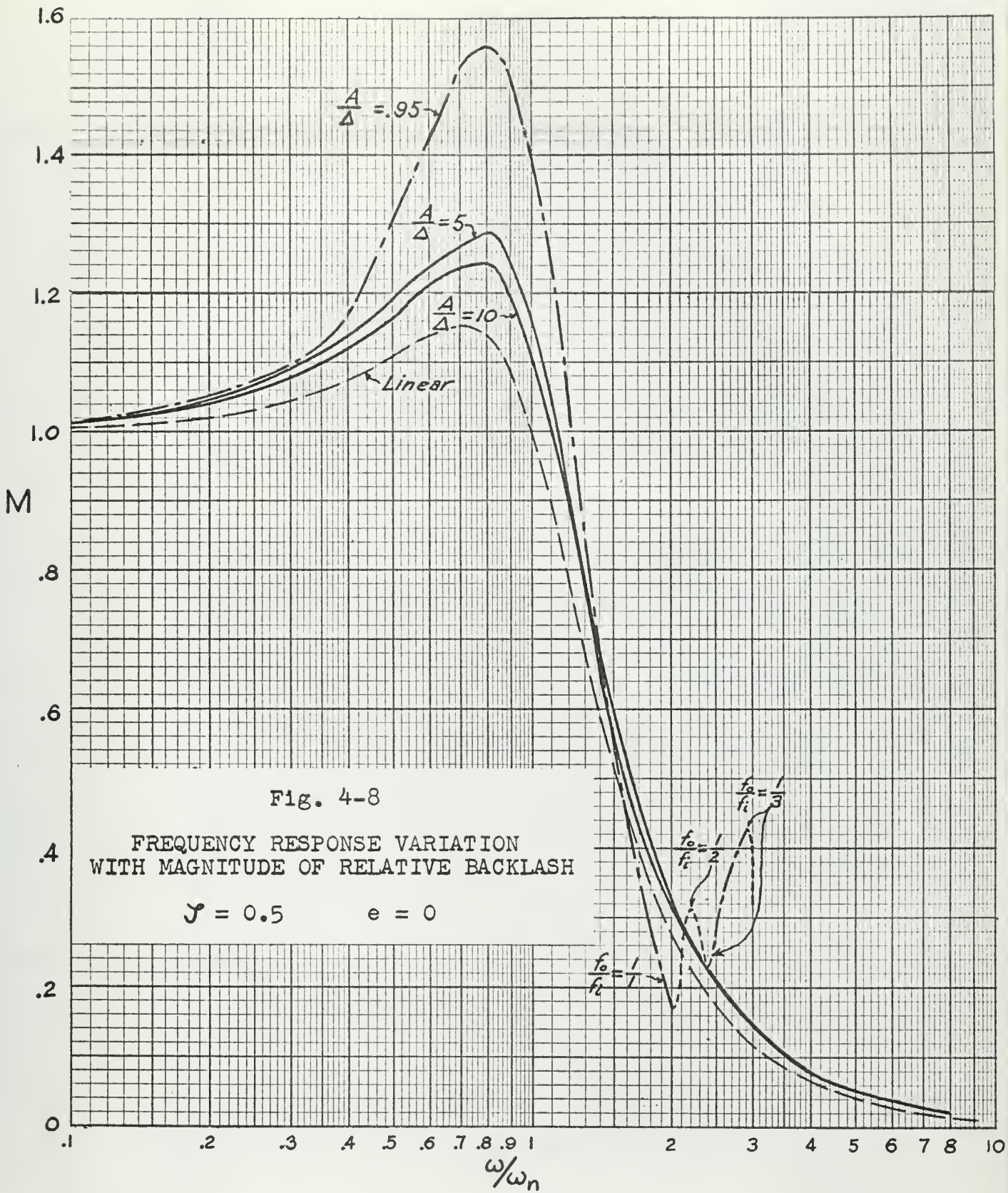WITH PLASTIC IMPACT

$\dfrac{A}{\Delta} = 0.95 \qquad e = 0$

49

Fig. 4-6

LINEAR SYSTEM FREQUENCY RESPONSE

$\triangle = 0 \qquad e = 0$

Fig. 4-7

COMPARISON OF M_p WITH LINEAR M_p FOR
VARYING AMOUNTS OF RELATIVE BACKLASH

$e = 0$

$\frac{M_p}{M_{p_{linear}}}$

$\frac{A}{\Delta}$

51

1.6

1.4

1.2

1.0

M

.8

.6

.4

.2

0

$\frac{A}{\Delta} = .95$

$\frac{A}{\Delta} = 5$

$\frac{A}{\Delta} = 10$

Linear
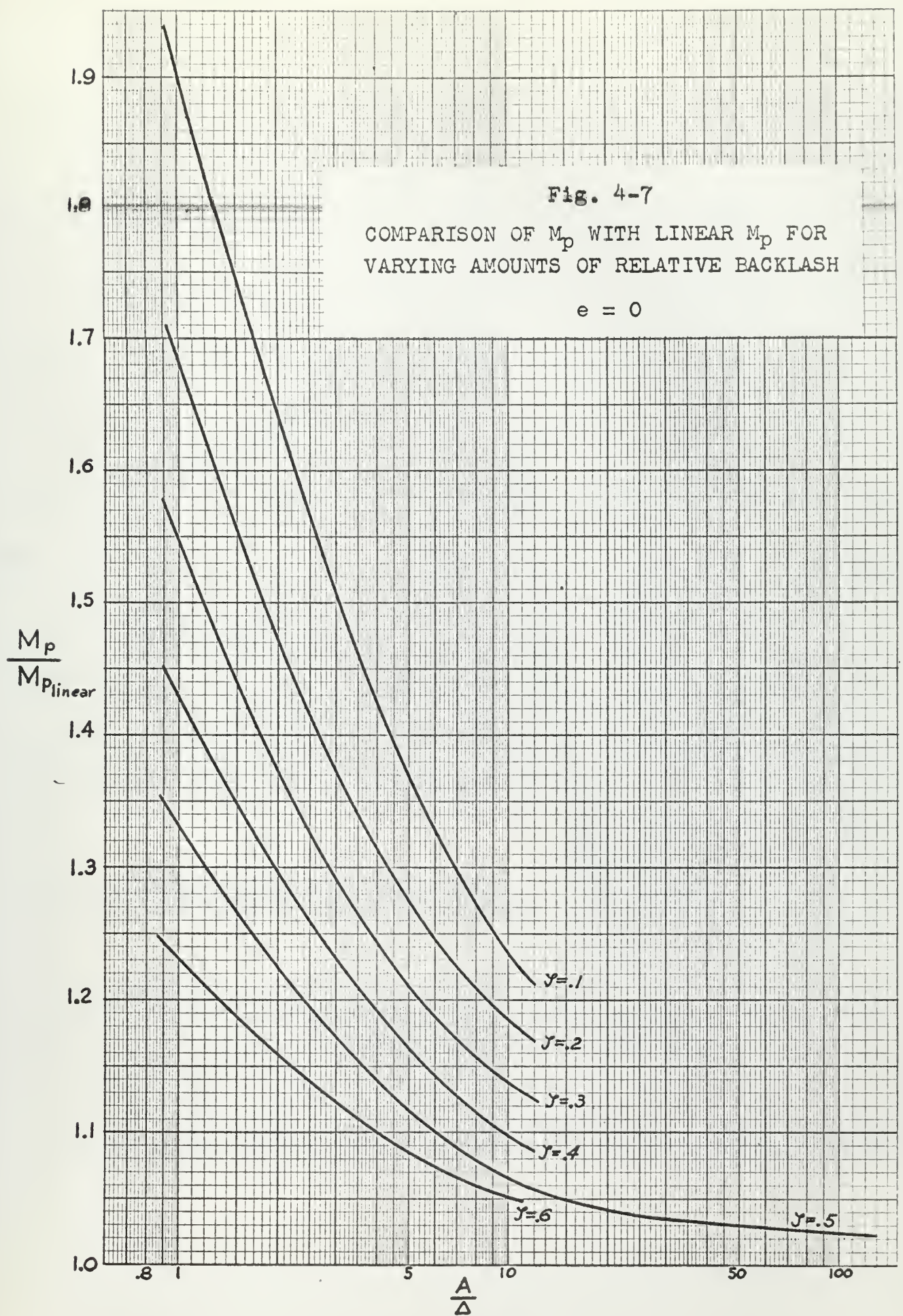
Fig. 4-8

FREQUENCY RESPONSE VARIATION
WITH MAGNITUDE OF RELATIVE BACKLASH

$\mathcal{J} = 0.5$ $e = 0$

$\frac{f_o}{f_i} = \frac{1}{3}$

$\frac{f_o}{f_i} = \frac{1}{2}$

$\frac{f_o}{f_i} = 1$

.1   .2   .3   .4 .5 .6 .7 .8 .9 1   2   3   4   5 6 7 8   10

ω/ω_n

52

Fig. 4-9

OUTPUT WAVE SHAPES

$\zeta = .5$ $A/\Delta = .95$ $e = 0$

a. $\omega = 1.8$, $f_0/f_1 = 1/1$

TIME, SECONDS

b. $\omega = 1.9$, $f_0/f_1 = 1/1$

53

Fig. 4-10

OUTPUT WAVE SHAPES

$\zeta = .5$ $A/\Delta = .95$ $e = 0$

a. $\omega = 2.0$, $f_0/f_1 = 1/1$

b. $\omega = 2.1$, $1/2 < f_0/f_1 < 1/1$

54

OUTPUT WAVE SHAPES

$\zeta = .5$ $A/\Delta = .95$ $e =$

a. $\omega = 2.2$, $f_0/f_1 = 1/2$

b. $\omega = 2.3$, $1/3 < f_0/f_1 < 1/2$

55

Fig. 4-12

OUTPUT WAVE SHAPES

$\zeta = .5$ $A/\Delta = .95$ $e = 0$

a. $\omega = 2.4$, $f_0/f_1 = 1/3$

TIME, SECONDS

b. $\omega = 2.5$, $f_0/f_1 = 1/3$

56

Fig. 4-13

OUTPUT WAVE SHAPES

$\zeta = .5$ $A/\Delta = .95$ $e = 0$

a. $\omega = 2.6$, $f_0/f_1 = 1/3$

b. $\omega = 2.7$, $f_0/f_1 = 1/3$

57

Fig. 4-14

OUTPUT WAVE SHAPES

$\zeta = .5$ $A/\Delta = .95$ e =

a. $\omega = 2.8$, $f_0/f_1 = 1/3$

TIME, SECONDS

b. $\omega = 2.9$, $f_0/f_1 = 1/3$

58

Fig. 4-15

OUTPUT WAVE SHAPE

$\zeta = .5$ $A/\Delta = .95$ $e = 0$

$\omega = 3.0$, $f_o/f_1 = 1/3$ (when output is steady)

TIME, SECONDS

Fig. 4-16

OUTPUT WAVE SHAPES
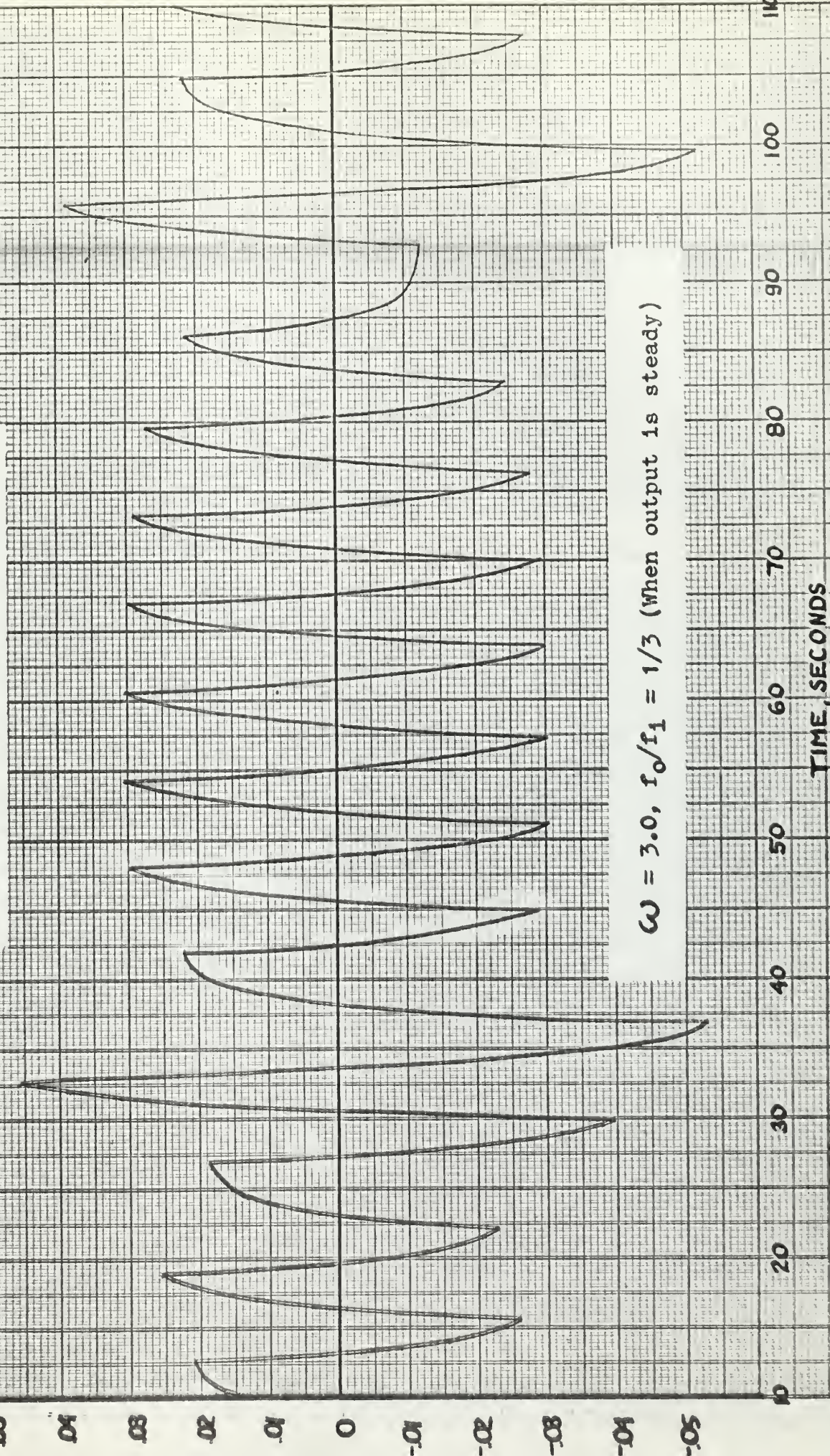
$\zeta = .5$ $A/\Delta = .95$ $e = 0$

a. $\omega = 3.1$, $f_0/f_1 = 1/3$ (When output is steady

b. $\omega = 4.0$, $1/5 < f_0/f_1 < 1/4$

Fig. 4-17

OUTPUT WAVE SHAPE

$\zeta = .5$ $A/\Delta = .95$ $e = 0$

$\omega = 5.0,$ $f_0/f_1 < 1/6$

OUTPUT POSITION, e, RADIANS
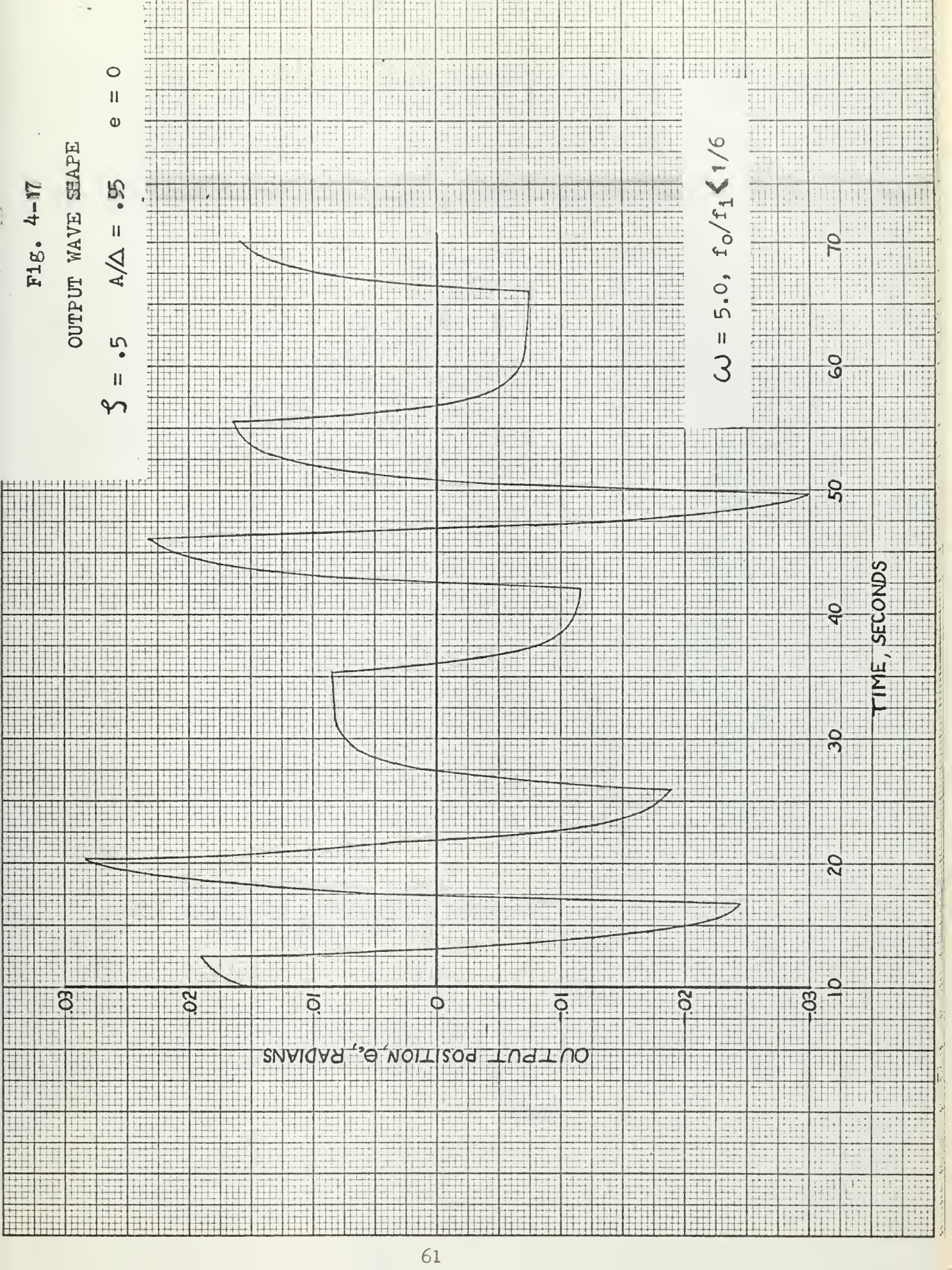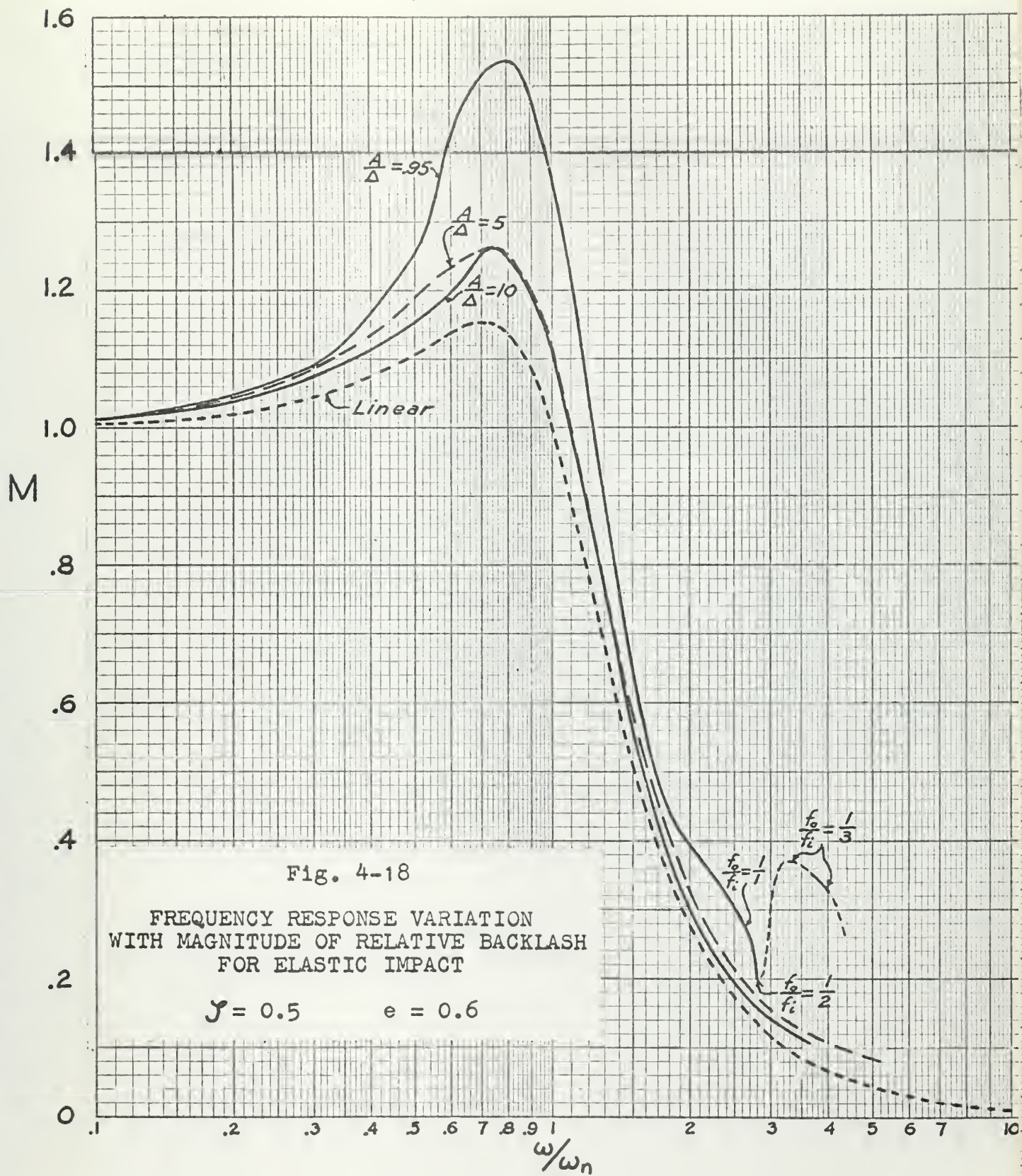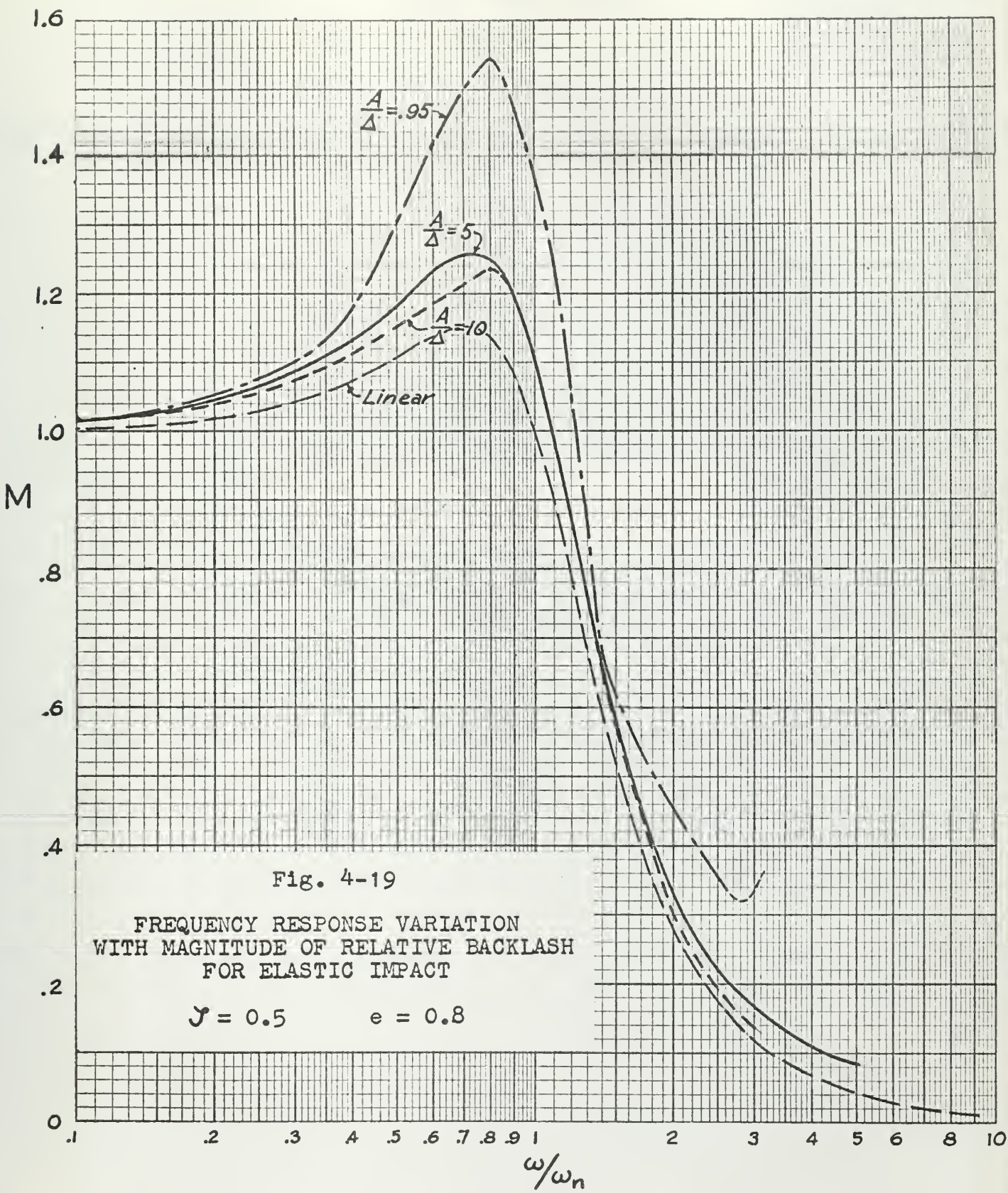
TIME, SECONDS

61

Fig. 4-18

FREQUENCY RESPONSE VARIATION
WITH MAGNITUDE OF RELATIVE BACKLASH
FOR ELASTIC IMPACT

$\gamma = 0.5$ $\qquad$ $e = 0.6$

Fig. 4-19

FREQUENCY RESPONSE VARIATION
WITH MAGNITUDE OF RELATIVE BACKLASH
FOR ELASTIC IMPACT

$\mathcal{J} = 0.5$ $e = 0.8$

63

Fig. 4-20

OUTPUT WAVE SHAPES

$\zeta = .5$ $A/\Delta = .95$ $e = .6$

a. $\omega = 2.7$, $f_o/f_1 = 1/1$

b. $\omega = 2.9$, $1/2 < f_o/f_1 < 1/1$

64

Fig. 4-21

OUTPUT WAVE SHAPES

$S = .5$ $A/\Delta = .95$ $e = .6$

a. $\omega = 2.8$, $1/1 < f_0/f_1 < 1/2$

TIME, SECONDS

OUTPUT POSITION, θ_c, RADIANS

b. $\omega = 3.0$, $1/2 < f_0/f_1 < 1/3$

Fig. 4-22

OUTPUT WAVE SHAPES

$\zeta = .5$ $A/\Delta = .95$ $e = .6$

a. $\omega = 3.2$, $1/2 > f_0/f_1 > 1/3$

b. $\omega = 3.4$, $f_0/f_1 = 1/3$

Fig. 4-23

OUTPUT WAVE SHAPES

$\zeta = .5$ $A/\triangle = .95$ $e = .6$

a. $\omega = 3.7$, $f_0/f_i = 1/3$

b. $\omega = 4.0$, $f_0/f_i = 1/3$

67
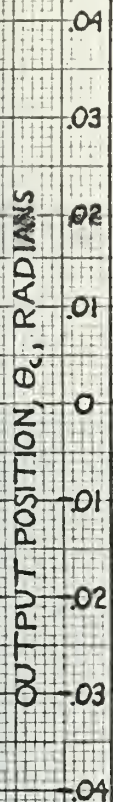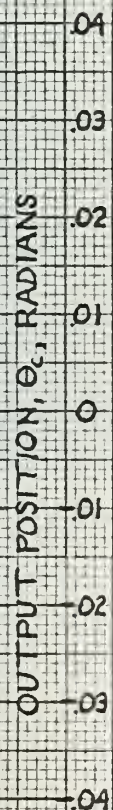
Fig. 4-24

OUTPUT WAVE SHAPE

$\zeta = .5$ $A/\Delta = .95$ $e = .6$

$\omega = 4.3$, $f_0/f_1 < 1/3$

OUTPUT POSITION, θ_c, RADIANS

TIME, SECONDS

68

Fig. 4-25

RESPONSE WITH LOW DAMPING RATIO
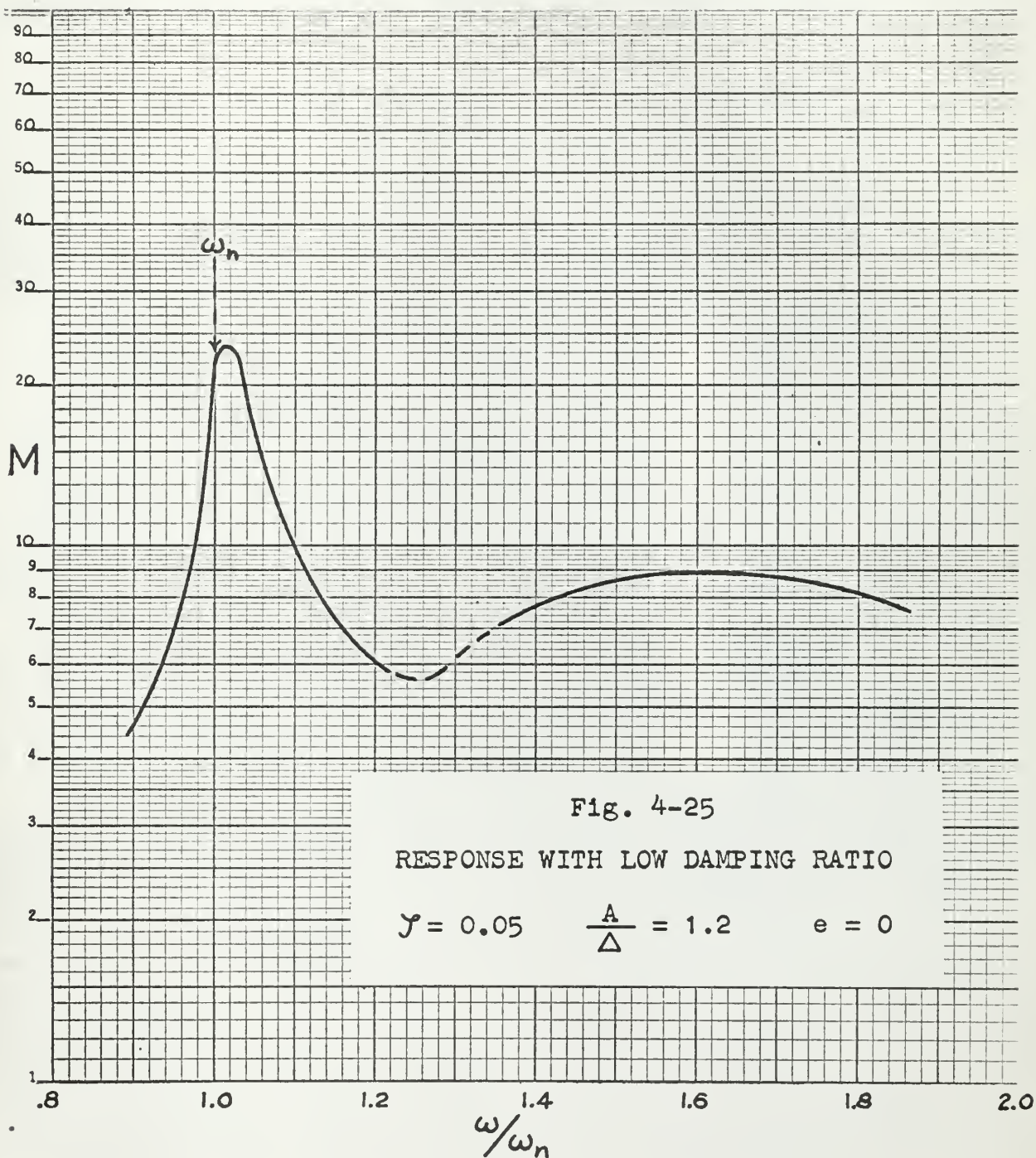
$\gamma = 0.05$ $\dfrac{A}{\Delta} = 1.2$ $e = 0$

Fig. 4-26
OUTPUT WAVE SHAPE
$\zeta = .05$ $A/\Delta = 1.2$ $e = 0$

$\omega = .95, f_0/f_1 = 1/1$

OUTPUT POSITION, θ_c, RADIANS
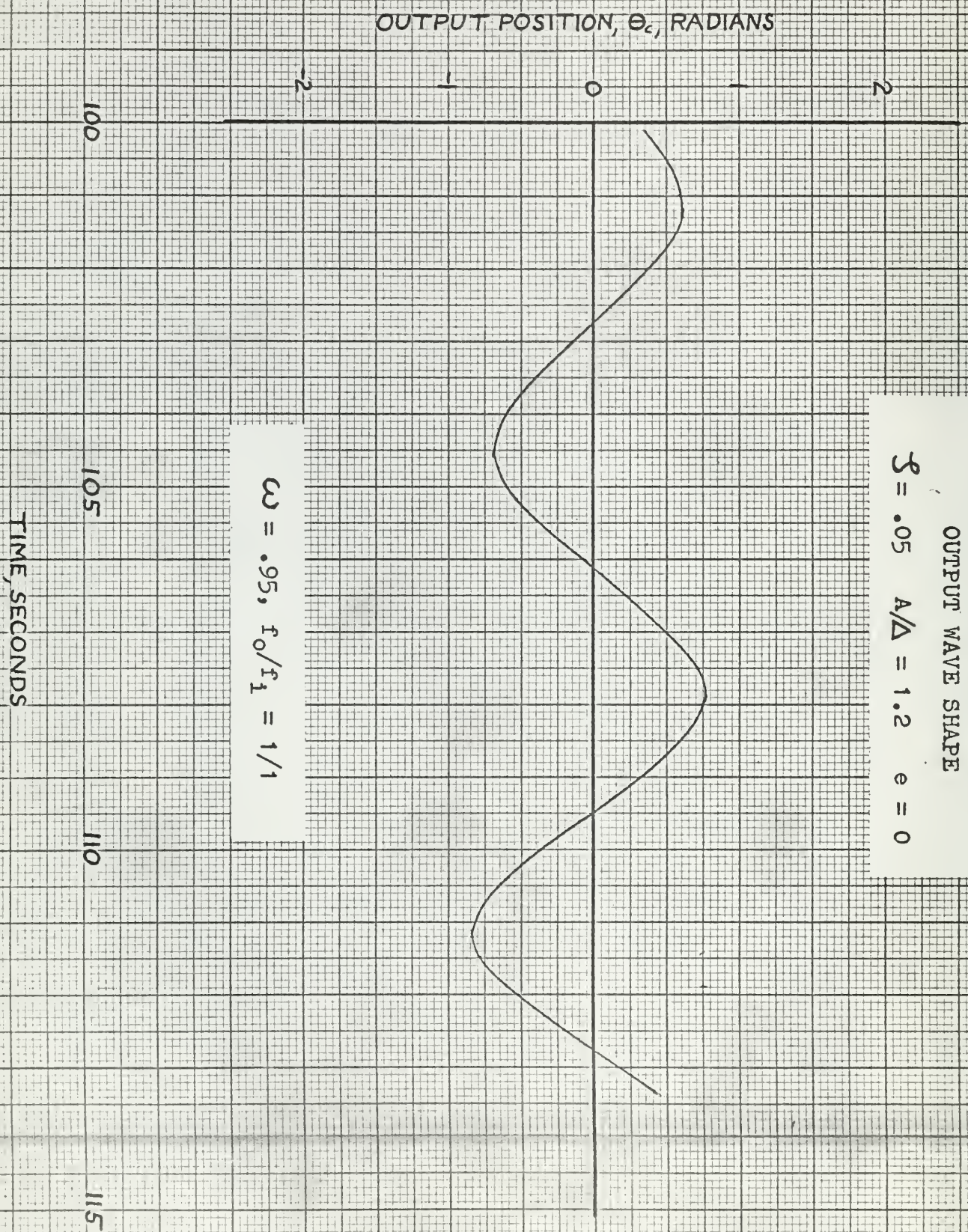
TIME, SECONDS

Fig. 4-27

OUTPUT WAVE SHAPE

$\delta = .05$ $A/\Delta = 1.2$ $e = 0$

$\omega = 1.0$, $f_0/f_1 = 1/1$

TIME, SECONDS

OUTPUT POSITION, θ, RADIANS

71
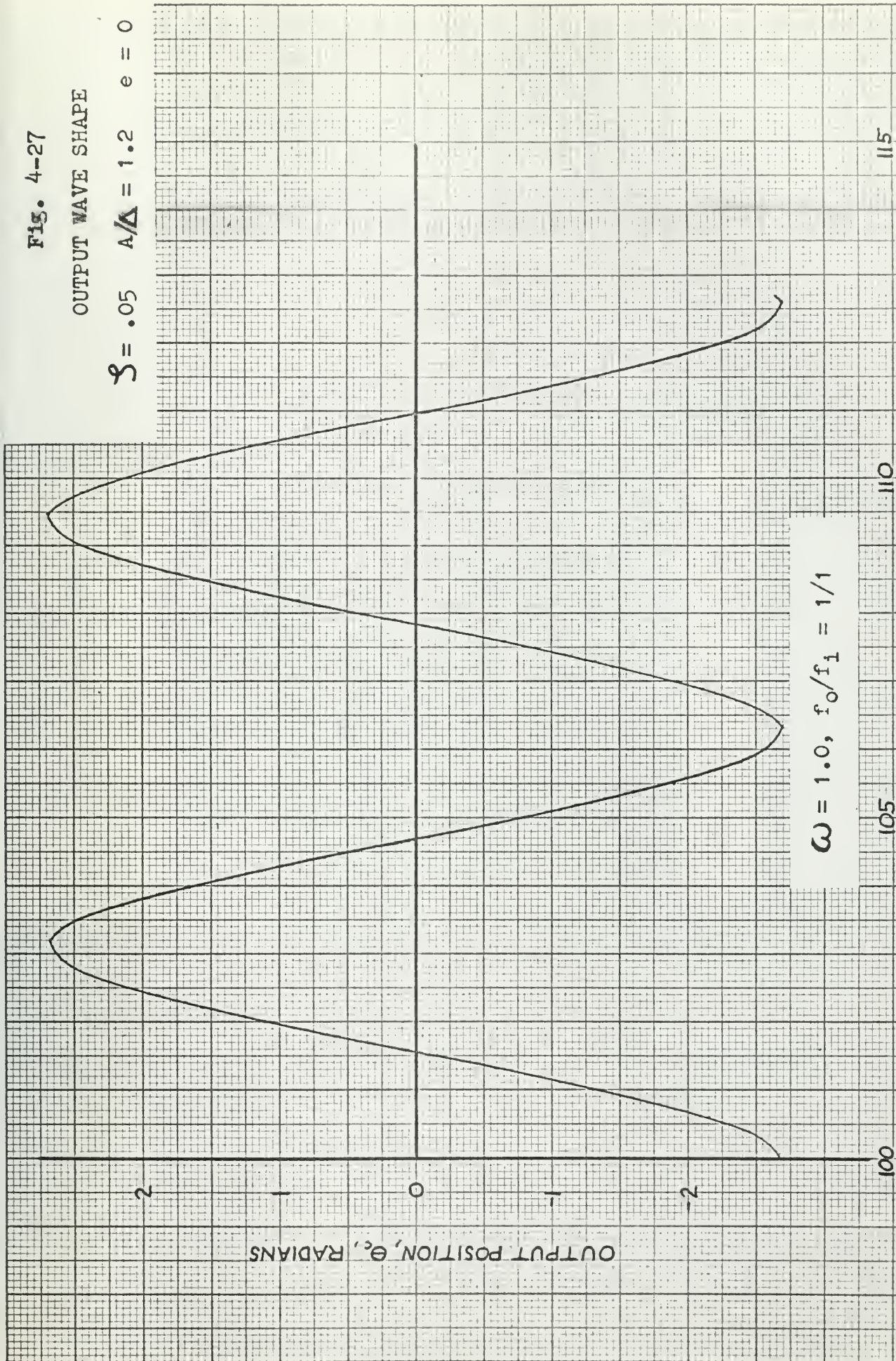
Fig. 4-28

OUTPUT WAVE SHAPES

$\zeta = .05 \quad A/\Delta = 1.2 \quad e = 0$

$\omega = 1.2, \quad 1/2 < f_0/f_1 < 1/1$

TIME, SECONDS

OUTPUT POSITION, θ, RADIANS
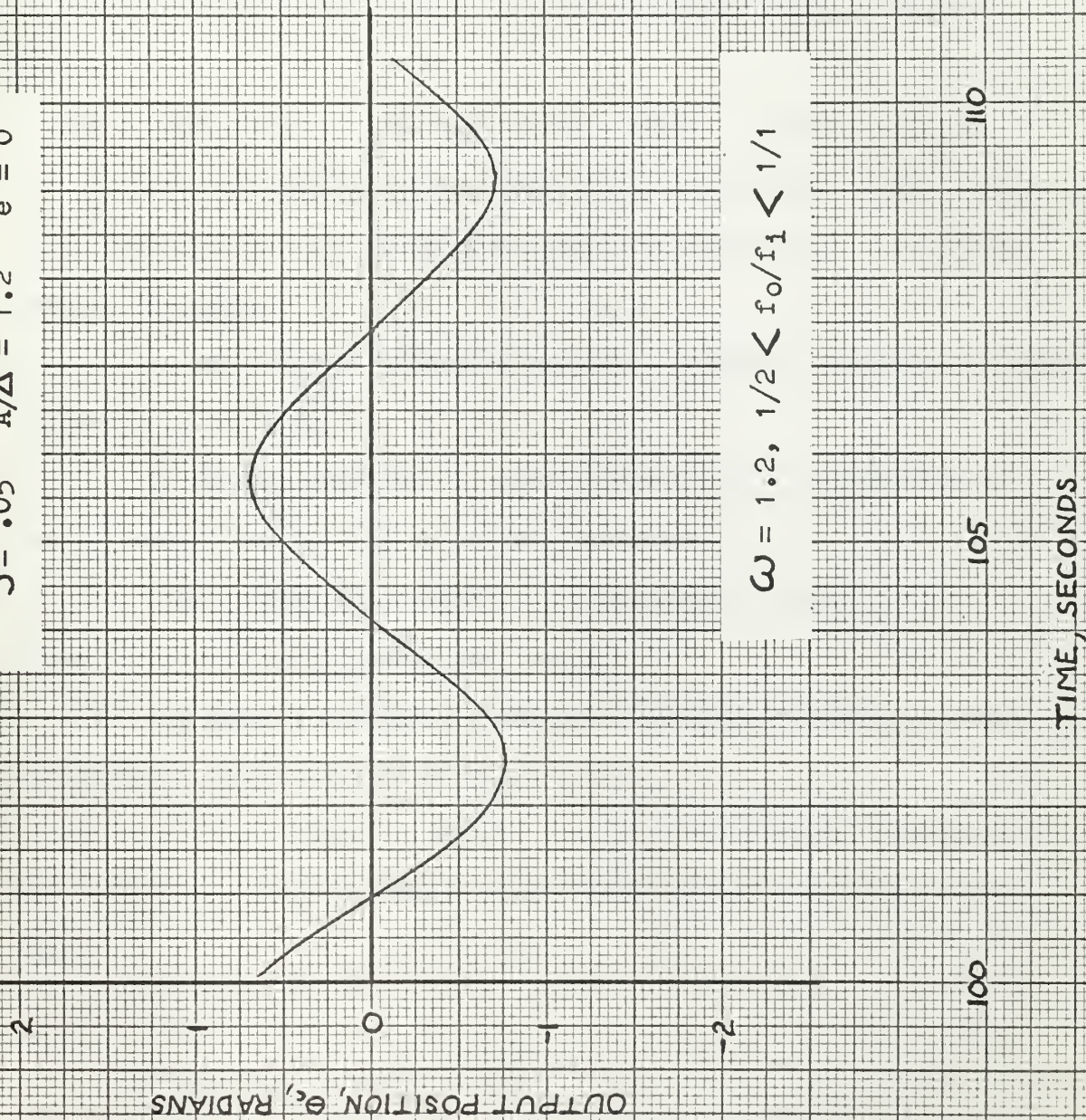
5. CONCLUSIONS

Based on the findings of this investigation, the following conclusions are made:

1. The system frequency response remains unchanged if A and Δ are varied proportionally, with all other parameters constant.

2. The presence of backlash in the system has an effect similar to lowering the damping ratio of the system.

3. The effect of backlash is more pronounced at lower damping ratios.

4. Increasing the backlash causes a more oscillatory response.

5. With a very low damping ratio and a small value of A/Δ , the first resonant peak can occur at a frequency greater than the undamped natural frequency.

6. At sub-harmonic resonance the ratio of input frequency to output frequency is an integer.

7. The output magnitude is erratic when the input frequency is not an integer multiple of the output frequency.

8. The odd sub-harmonics are more pronounced; and with elastic impact, the even sub-harmonic does not appear.

9. The lower the damping ratio, the lower the frequency at which sub-harmonic resonance will occur.

10. With all other parameters constant, sub-harmonic resonance will occur at a lower frequency with plastic impact than with elastic impact.

11. The effect of elastic impact is to reduce the effect of back-lash.

12. With a coefficient of restitution of either 0.6 or 0.8, the frequency response of the system is essentially the same.

13. Combinations of low damping ratio and high frequency require excessive computer time to obtain the frequency response.

14. When a limit cycle exists (Ref. 2), an oscillation at the undamped natural frequency of the system is superimposed on the output motion.

REFERENCES

1. New, N. C., "Effects of Backlash in the Second Order Servo",
    Unpublished Masters Thesis, U. S. Naval Postgraduate School, 1960.

2. Anderson, N. O. and Luckett, T. W., "Steady State Response of a
    Second Order Servomechanism with Backlash and Resilience in the
    Gears Between Motor and Load", Unpublished Masters Thesis, U. S.
    Naval Postgraduate School, 1961.

3. Andrews, C. E. and Kelley, R. A., "Effects of Maximum Overshoot
    and Settling Time when Backlash is Present in a Second Order
    Servomechanism", Unpublished Masters Thesis, U. S. Naval Post-
    graduate School, 1961.

BIBLIOGRAPHY

Housner, G. W. and Hudson, D. E., <u>Applied Mechanics Dynamics</u>,
    D. Van Nostrand Co., Inc., Princeton, N. J., 1959.

Johnson, E. C., "Sinusoidal Analysis of Feedback-Control Systems
    Containing Nonlinear Elements", A.I.E.E. Transactions
    (Applications and Industry), July 1952.

Lance, G. N., <u>Numerical Methods for High Speed Digital Computers</u>,
    Iliffe & Sons Ltd., London, 1960.

Thaler, G. J. and Pastel, M. P., <u>Analysis and Design of Nonlinear</u>
    <u>Feedback Control Systems</u>, McGraw-Hill Book Co., Inc., New York,
    1962.

Truxel, G. J., <u>Control Engineers Handbook</u>, McGraw-Hill Book Co., Inc.,
    New York, 1958.

Tustin, A., "The Effects of Backlash and of Speed-Dependent Friction
    on the Stability of Closed-Cycle Control Systems", Journal of
    The Institution of Electrical Engineers (Automatic Regulators
    and Servo Mechanisms), Vol. 94, Part IIA, 1947.

<u>Characteristics of the Model 1604 Computer</u>, Publication No. 018a,
    Control Data Corporation, 1959.

<u>Fortran System for the Control Data 1604 Computer</u>, Publication
    No. 087A, Control Data Corporation, 1961.

78

79
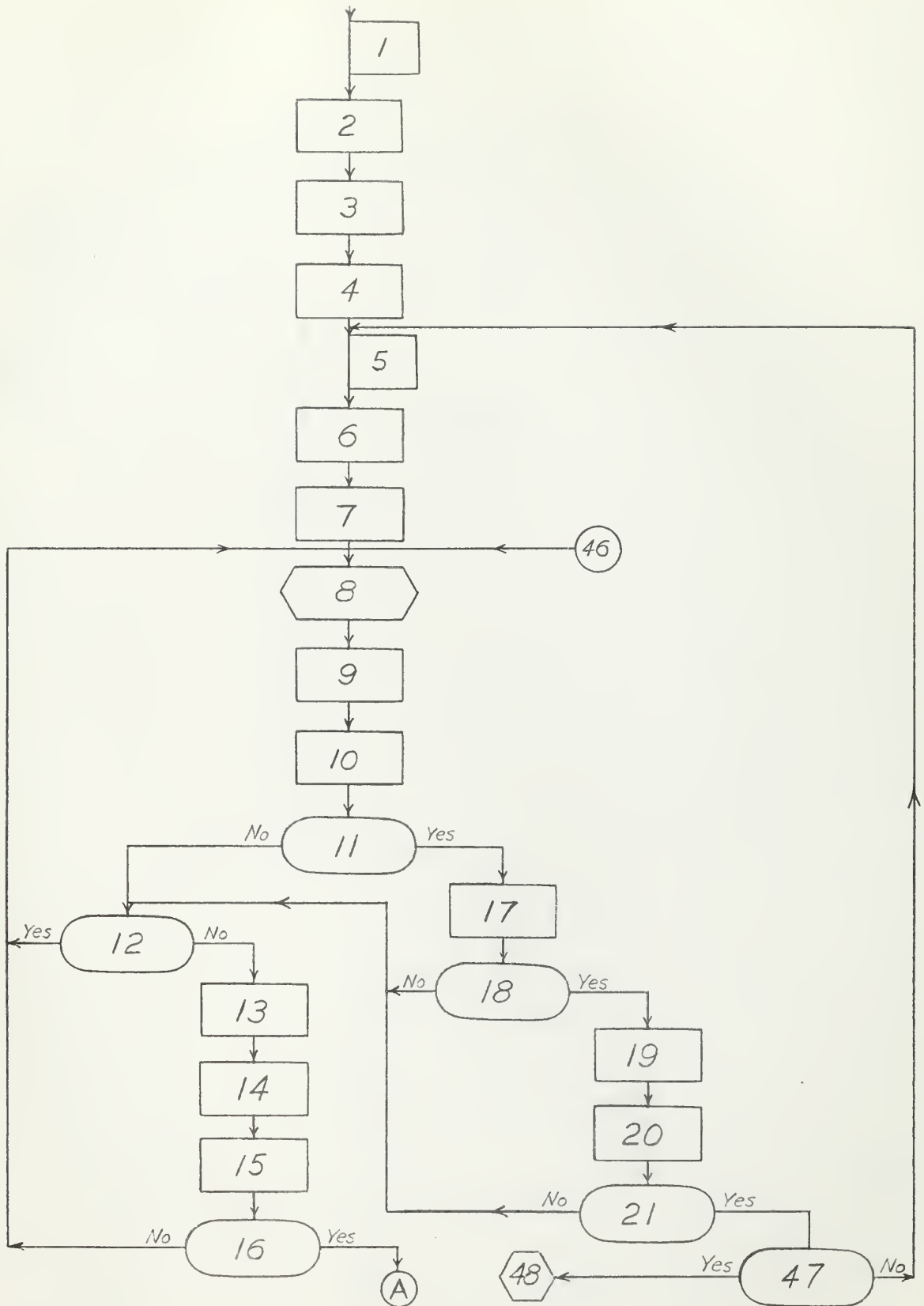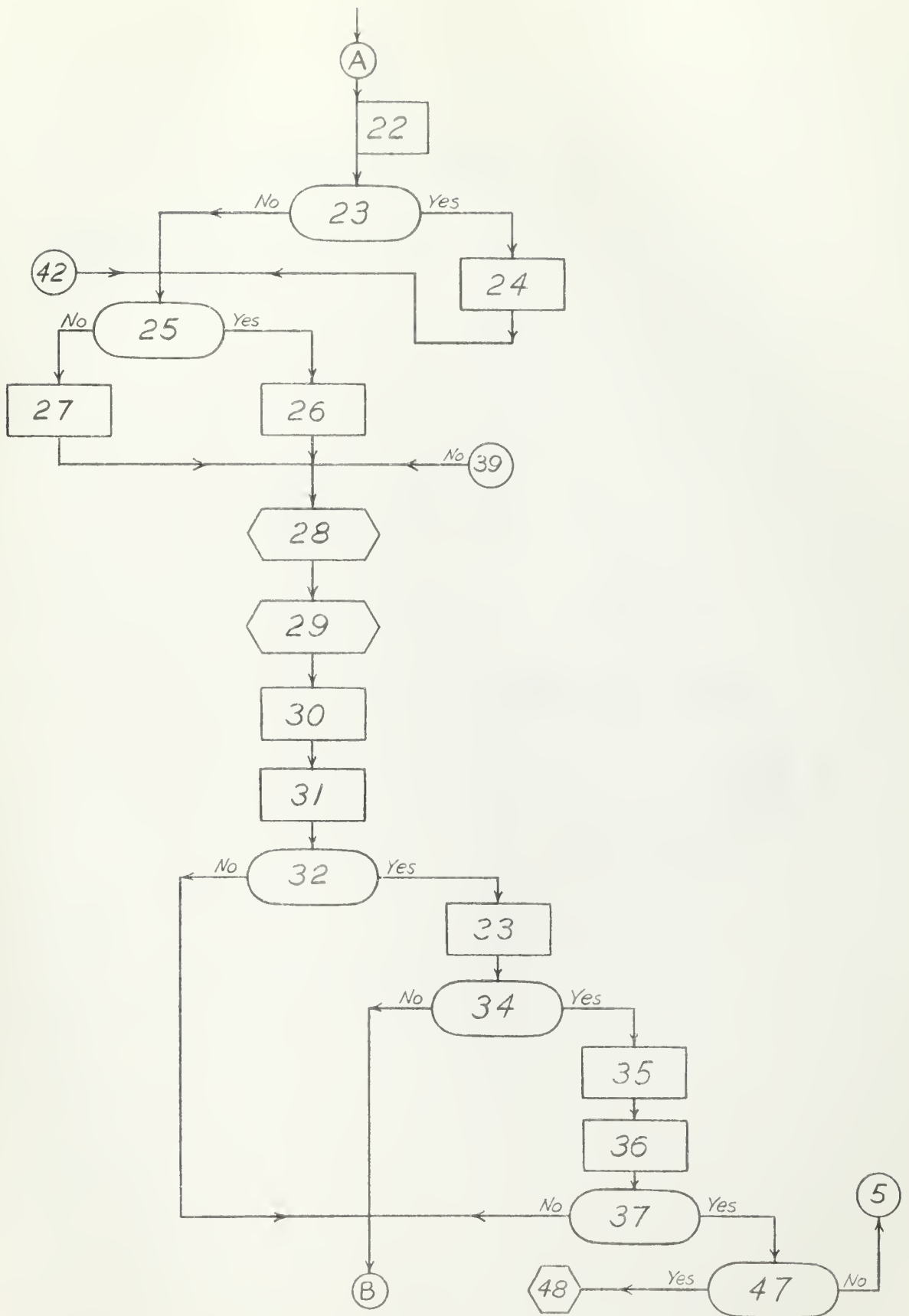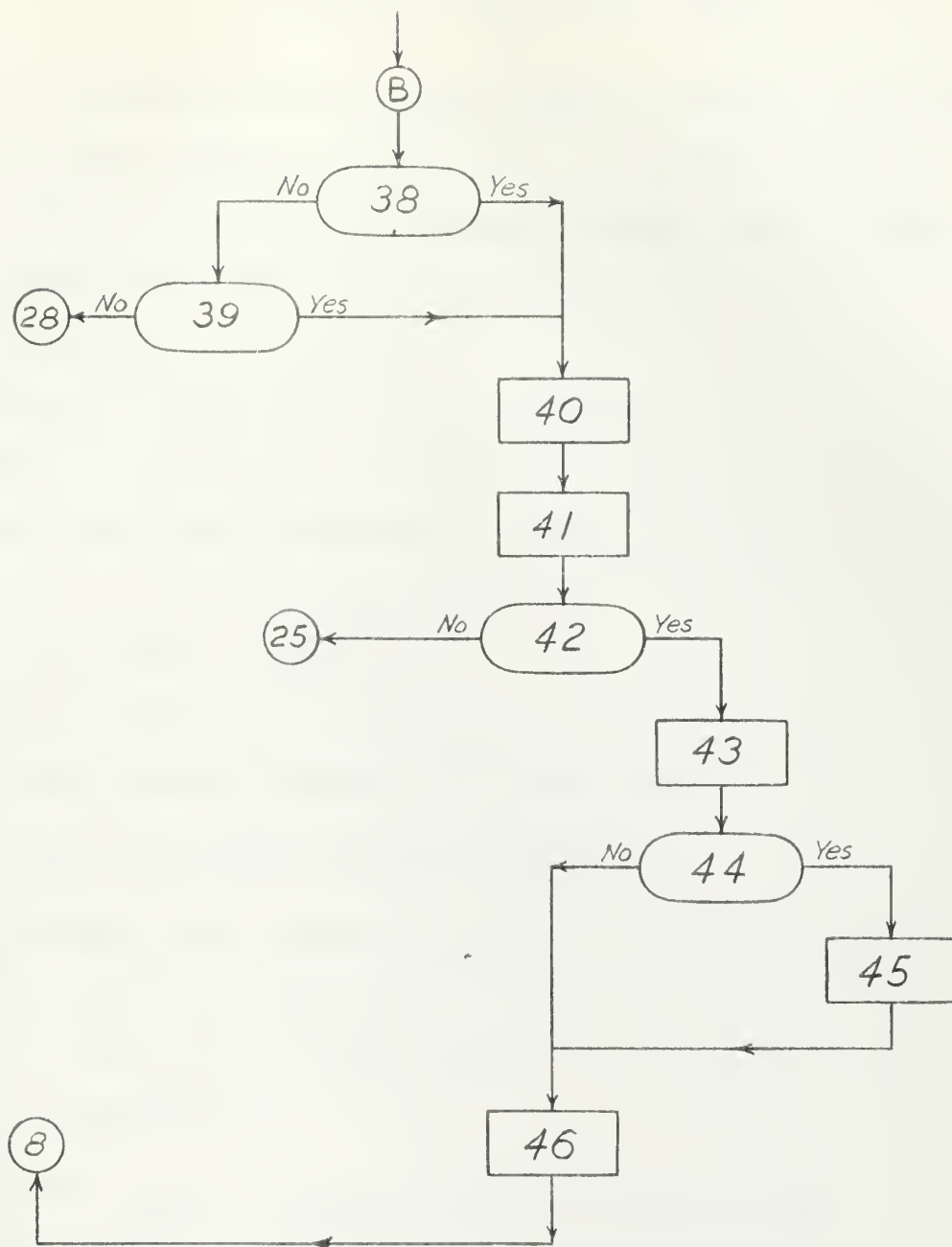
EXPLANATION OF FLOW CHART NUMBERS

1. Set initial conditions and assign values to constants and parameters of system equations: i.e., $\mathcal{Y}$, f_M, f_L, A, Δ, e, K, ρ, ω_n, Problem time for delay of five time constants, number of input cycles desired after five time constants.

2. *Print heading for results.

3. *Print run number and values of e, $\mathcal{Y}$ and A.

4. *Print column headings for Time, θ_L, $\dot{\theta}_L$, θ_M, $\dot{\theta}_M$ and θ_R.

5. Set first initial conditions for combined differential equation:
$$\text{Time} = 0, \quad \theta_c = 0, \quad \dot{\theta}_c = 0$$

6. Select values of ω and Δt.

7. *Print values of ω, Δt, and J_L.

8. Solve differential equation for combined operation
$$\ddot{\theta}_c + 2\mathcal{Y}\omega_n\dot{\theta}_c + \omega_n^2\theta_c = \omega_n^2 A \sin\omega t$$

9. Increment time by integration interval $t \rightarrow t + \Delta t$.

10. Calculate value of input θ_R.

11. Does time equal five time constants?

12. Is backlash zero?

13. Solve for
$$\ddot{\theta}_c = -2\mathcal{Y}\omega_n\dot{\theta}_c - \omega_n^2\theta_c + \omega_n^2 A \sin\omega t$$

14. Calculate $N_c = \ddot{\theta}_c / \dot{\theta}_c$

15. Calculate $N_L = - f_L / J_L$

16. Does $N_c = -N_L$?

17. Count a time increment Δt.

18. Gone through 100 Δt's?

19. Set Δt count to zero.

20. *Print values of Time, θ_c, $\dot{\theta}_c$ and θ_R.

21. Does time equal five time constants plus time for desired number of input cycles after transient period?

22. Set initial conditions for second and third differential equations.

23. Does time equal five time constants?

24. *Print values of Time, θ_c, $\dot{\theta}_c$ and θ_R.

25. Are gear teeth separating from original contact position plus Δ?

26. Calculate $\theta_M = \dfrac{\theta_L - \Delta}{\rho}$

27. Calculate $\theta_M = \dfrac{\theta_L}{\rho}$

28. Solve differential equation for motor alone

$$\ddot{\theta}_M + \frac{f_M}{J_M}\dot{\theta}_M + \frac{K}{J_M}\theta_L = \frac{K}{J_M} A \sin \omega t$$

29. Solve differential equation for load alone

$$\ddot{\theta}_L + \frac{f_L}{J_L}\dot{\theta}_L = 0$$

30. Increment time $t \rightarrow t + \Delta t$.

31. Calculate value of input θ_R.

32. Does time equal five time constants?

33. Count a time increment Δt.

34. Gone through 100 Δt's?

35. Set Δt count to zero.

36. *Print values of Time, θ_L, $\dot{\theta}_L$, θ_M, $\dot{\theta}_M$ and θ_R.

81

37. Does time equal five time constants plus time for desired number of input cycles after transient period?

38. Are gear teeth touching in initial contact position?

39. Are gear teeth touching in initial position plus Δ?

40. Calculate load bounce velocity $\dot{\theta}_L'$

$$\dot{\theta}_L' = \frac{J_M}{J_M + \rho^2 J_L} \left[\rho \dot{\theta}_M (1 + e) + \dot{\theta}_L \left(\frac{\rho^2 J_L}{J_M} - e \right) \right]$$

41. Calculate motor bounce velocity $\dot{\theta}'$

$$\dot{\theta}_M' = \frac{\dot{\theta}_L' - e \rho \dot{\theta}_M + e \dot{\theta}_L}{\rho}$$

42. Do gear teeth stay together?

43. Set initial conditions for combined differential equation.

44. Does time equal five time constants?

45. *Print values of Time, θ_L, $\dot{\theta}_L$, θ_M, $\dot{\theta}_M$ and θ_R.

46. Go to combined differential equation.

47. Completed calculation for all values of ω?

48. Stop.

* "Print" refers to putting the indicated items or their values onto magnetic tape for later printing.

APPENDIX B

COMPUTER FORTRAN SOURCE PROGRAM

```
      PROGRAM BLASH
      DIMENSION DM(3), DL(3), W(28), TINT(28), Y1(2), Y2(2), Y3(2)
      COMMON ZETA, WN, A, OMEGA, FL, DLOAD, FM, DMOTOR, GC, THEL
      ZETA = 0.5
      FL = 0.4
      FM = 0.6
      DELAY = 10.0
      A = 1.0
      BL = 0.1
      E = 0.0
      CYC = 6.3
      GC = 1.0
      RHO = 1.0
      WN = 1.0
      EPS = .45474735E-12
    1 FORMAT (3F10.1)
      READ INPUT TAPE 7, 1 (DL(J), J = 1, 3)
      READ INPUT TAPE 7, 1 (DM(J), J = 1, 3)
   23 FORMAT (7F10.2)
      READ INPUT TAPE 7, 23 (W(I), I = 1, 28)
   24 FORMAT (6F12.10)
      READ INPUT TAPE 7, 24 (TINT(I), I = 1, 28)
   50 FORMAT (58HIRESULTS OF NONLINEAR SERVO WITH BACKLASH    GRAHAM / LL
     1OYD)
      WRITE OUTPUT TAPE 8, 50
    2 OFORMAT (23HOPRODUCTION RUN 19 E = ,
     1F3.1, 3X, 7HZETA = , F4.2, 3X, 4HA = , F6.3)
      WRITE OUTPUT TAPE 8, 2, E, ZETA, A
    3 OFORMAT (5X, 4HTIME, 12X, 9HOUT POSIT, 13X, 7HOUT VEL, 9X, 11HMOTOR
     1 POSIT, 11X, 9HMOTOR VEL, 11X, 9HINPUT POS)
      WRITE OUTPUT TAPE 8, 3
      DO 19 J = 2,2
      DO 19 I = 8, 9
      PAUSE
      DELT = TINT(I)
      OMEGA = W(I)
      DLOAD = DL(J)
      DMOTOR = DM(J)
      FINI = CYC/W(I)
      T = 0.0
      Y1(1) = 0.0
      Y1(2) = 0.0
   22 OFORMAT (8HOOMEGA = ,F5.1, 5X, 11HINTERVAL = ,F12.10, 5X,
     115HLOAD INERTIA = ,F2.1)
      WRITE OUTPUT TAPE 8, 22, W(I), TINT(I), DL(J)
      M = 0
    5 CALL RKUTTA1 (2, T, Y1, DELT)
      T = T + DELT
      FORCE = A*SINF(OMEGA*T)
      THEC = Y1(1)
      THECD = Y1(2)
      IF(T - DELAY) 26, 26, 30
   30 M = M+ 1
      IF (M - 100) 26, 27, 27
   27 M = 0
      WRITE OUTPUT TAPE 8, 4, T, THEC, THECD, FORCE
    4 FORMAT (F10.3, 2F20.5, 40X, F20.5)
      IF (T - DELAY - FINI) 26, 19, 19
   26 IF (BL) 5, 5, 21
   21 THECDD = -2.0*ZETA*WN*THECD - WN*WN*THEC + WN*WN*A*SINF(W(I)*T)
      SLOPEC = THECDD/THECD
      SLOPEL = -FL/DL(J)
      IF (SLOPEC - SLOPEL) 6, 6, 5
    6 THEL = THEC
      Y3(1) = THEC
      Y2(2) = THECD
      Y3(2) = THECD
      IF (T - DELAY) 16, 16, 33
   33 WRITE OUTPUT TAPE 8, 4, T, THEC, THECD, FORCE
   16 IF (Y3(2)) 7, 8, 8
    7 Y2(1) = (Y3(1) - BL)/ RHO
      GO TO 9
```

```
   8   Y2(1) = Y3(1)/RHO
   9   CALL RKUTTA2 (2, T, Y2, DELT)
       THEM = Y2(1)
       THEMD = Y2(2)
       CALL RKUTTA3 (2, T, Y3, DELT)
       THEL = Y3(1)
       THELD = Y3(2)
       T = T + DELT
       FORCE = A*SINF(OMEGA*T)
       IF (T - DELAY) 28, 28, 31
  31   M = M + 1
       IF (M - 100) 28, 29, 29
  29   M = 0
  10   FORMAT (F10.3, 5F20.5)
       WRITE OUTPUT TAPE 8, 10, T, THEL, THELD, THEM, THEMD, FORCE
       IF (T - DELAY - FINI) 28, 19, 19
  28   IF (THEL - RHO*THEM) 13, 13, 11
  11   IF (THEL - RHO*THEM - BL) 12, 13, 13
  12   GO TO 9
       IF (E) 17, 17, 13
  13   BOLVEL = (DM(J) / (DM(J) + RHO * RHO * DL(J))) *(RHO * THEMD
      1*(1.0 + E) + THELD * ((RHO * RHO * DL(J)) /DM(J) - E))
       BOMVEL = (BOLVEL - E*RHO*THEMD + E*THELD)/RHO
       THELD = BOLVEL
       THEMD = BOMVEL
       Y2(2) = THEMD
       Y3(2) = THELD
       DIFVEL = RHO*THEMD - THELD
       IF (DIFVEL) 14, 15, 15
  14   DIFVEL = -DIFVEL
  15   IF (DIFVEL - EPS) 17, 17, 16
  17   Y1(1) = THEL
       Y1(2) = THELD
  35   IF (T - DELAY) 34, 34, 18
  18   WRITE OUTPUT TAPE 8, 10, T, THEL, THELD, THEM, THEMD, FORCE
  34   GO TO 5
  19   CONTINUE
       END FILE 8
       STOP
       END

       SUBROUTINE RKUTTA1(NUMBER,XVAR,YVARS,STEP)
       DIMENSION YVARS(30),AK(4,30),DY(30),YC(30),C(4)
       COMMON ZETA, WN, A, OMEGA, FL, DLOAD, FM, DMOTOR, GC, THEL
       C(1) = 0.0
       C(2) = 0.5
       C(3) = 0.5
       C(4) = 1.0
       DO 1 I=1,4
       XC=XVAR + C(I)*STEP
       DO 2 J=1,NUMBER
   2   YC(J) =YVARS(J) + C(I)*AK(I-1,J)
       CALL DERIV1(XC,YC,DY)
       DO 1 J=1,NUMBER
   1   AK(I,J) = STEP * DY(J)
       DO 3 J = 1,NUMBER
   3   YVARS(J) =YVARS(J) + (AK(1,J)+2.*AK(2,J)+2.*AK(3,J)+AK(4,J))/6.
       RETURN
       END

       SUBROUTINE DERIV 1 (T, Y, DY)
       DIMENSION Y(2), DY(2), W(28)
       COMMON ZETA, WN, A, OMEGA, FL, DLOAD, FM, DMOTOR, GC, THEL
       DY(1) = Y(2)
       DY(2) = WN*WN*A*SINF(OMEGA*T) - WN*WN*Y(1) - (2.0*ZETA*WN)*Y(2)
       RETURN
       END

       SUBROUTINE RKUTTA2(NUMBER,XVAR,YVARS,STEP)
       DIMENSION YVARS(30),AK(4,30),DY(30),YC(30),C(4)
       COMMON ZETA, WN, A, OMEGA, FL, DLOAD, FM, DMOTOR, GC, THEL
       C(1)=0.0
       C(2)=0.5
```

```
      C(3)=0.5
      C(4)=1.0
      DO 1 I=1,4
      XC=XVAR + C(I)*STEP
      DO 2 J=1,NUMBER
   2  YC(J) =YVARS(J) + C(I)*AK(I-1,J)
      CALL  DERIV2(XC,YC,DY)
      DO 1 J=1,NUMBER
   1  AK(I,J) = STEP * DY(J)
      DO 3 J = 1,NUMBER
   3  YVARS(J) =YVARS(J) + (AK(1,J)+2.*AK(2,J)+2.*AK(3,J)+AK(4,J))/6.
      RETURN
      END

      SUBROUTINE DERIV 2 (I, Y, DY)
      DIMENSION Y(2), DY(2), W(28), DM(3)
      COMMON ZETA, WN, A, OMEGA, FL, DLOAD, FM, DMOTOR, GC, THEL
      DY(1) = Y(2)
     0DY(2) = (GC / DMOTOR)*A*SINF(OMEGA*T) - (FM / DMOTOR)*Y(2) -
     1(GC / DMOTOR)*THEL
      RETURN
      END

      SUBROUTINE RKUTTA3(NUMBER,XVAR,YVARS,STEP)
      DIMENSION YVARS(30),AK(4,30),DY(30),YC(30),C(4)
      COMMON ZETA, WN, A, OMEGA, FL, DLOAD, FM, DMOTOR, GC, THEL
      C(1)=0.0
      C(2)=0.5
      C(3)=0.5
      C(4)=1.0
      DO 1 I=1,4
      XC=XVAR + C(I)*STEP
      DO 2 J=1,NUMBER
   2  YC(J) =YVARS(J) + C(I)*AK(I-1,J)
      CALL DERIV 3 (XC, YC, DY)
      DO 1 J=1,NUMBER
   1  AK(I,J) = STEP * DY(J)
      DO 3 J = 1,NUMBER
   3  YVARS(J) =YVARS(J) + (AK(1,J)+2.*AK(2,J)+2.*AK(3,J)+AK(4,J))/6.
      RETURN
      END

      SUBROUTINE DERIV 3 (T, Y, DY)
      DIMENSION Y(2), DY(2), W(28), DL(3)
      COMMON ZETA, WN, A, OMEGA, FL, DLOAD, FM, DMOTOR, GC, THEL
      DY(1) = Y(2)
      DY(2) = - (FL /DLOAD)*Y(2)
      RETURN
      END
      END
```

```
      .2              .5              .8
      .8              .5              .2
      .1              .2              .3          .4          .5          .6          .7
      .8              .9             1.0         1.2         1.4         1.7         2.0
     2.5             3.0             4.0         5.0         6.0         7.0         8.0
     9.0            10.0            20.0        30.0        40.0        50.0        60.0
.01             .005            .0033333333 .0025           .002          .0016666667
.0014285714 .00125             .0011111111 .001            .0008333333 .0007142857
.0005882353 .0005               .0004       .0003333333 .00025          .0002
.0001666667 .0001428571 .000125            .0001111111 .0001            .00005
.0000333333 .000025             .00002      .0000166667
```

85

RESULTS OF NONLINEAR SERVO WITH BACKLASH   GRAHAM / LLOYD

PRODUCTION RUN 19 E = .0   ZETA = .50   A = 1.000

TIME	OUT POSIT	OUT VEL	MOTOR POSIT	MOTOR VEL	INPUT POS
OMEGA = .8	INTERVAL = .0012500000	LOAD INERTIA = .5			
10.125	.71215	.73609			.96787
10.250	.80023	.67286			.94073
10.257	.80531	.66886			.93866
10.375	.88032	.60885	.87988	.59773	.90217
10.500	.95274	.55091	.94899	.50538	.85460
10.625	1.01828	.49848	1.00559	.39783	.79849
10.750	1.07757	.45105	1.04789	.27682	.73440
10.875	1.13123	.40812	1.07430	.14380	.66297
11.000	1.17977	.36929	1.08339	.00008	.58492
11.010	1.18345	.17725	1.08334	.17725	.57841
11.011	1.18367	.17627			.57759
11.125	1.20284	.16094	1.17452	-.01456	.50102
11.250	1.22198	.14563	1.18524	-.16318	.41212
11.375	1.23931	.13177	1.15370	-.34154	.31910
11.405	1.24321	-.12792	1.14281	-.12792	.29626
11.500	1.22739	-.20484			.22289
11.625	1.19562	-.30290			.12445
11.750	1.15185	-.39664			.02478
11.875	1.09667	-.48526			-.07515
12.000	1.03078	-.56804			-.17433
12.125	.95493	-.64431			-.27176
12.250	.87000	-.71344			-.36648
12.375	.77689	-.77489			-.45754
12.500	.67661	-.82818			-.54402
12.625	.57021	-.87283			-.62507
12.750	.45876	-.90868			-.69987
12.875	.34342	-.93530			-.76769
13.000	.22533	-.95254			-.82783
13.125	.10567	-.96043			-.87970
13.250	-.01437	-.95833			-.92278
13.375	-.13365	-.94786			-.95663
13.500	-.25077	-.92768			-.98094
13.625	-.36520	-.89854			-.99544
13.750	-.47524	-.86073			-.99997
13.875	-.58003	-.81468			-.99455
14.000	-.67858	-.76086			-.97913
14.125	-.76995	-.69281			-.95402
14.179	-.80680	-.67143			-.94025
14.250	-.85331	-.63428	-.75321	-.63007	-.91933
14.375	-.92276	-.57392	-1.02674	-.54355	-.87545
14.500	-.99703	-.51930	-1.08844	-.44117	-.82283
14.625	-1.05880	-.46988	-1.13645	-.32461	-.76193
14.750	-1.11470	-.42517	-1.16912	-.19557	-.69353
14.875	-1.16527	-.35471	-1.18499	-.05590	-.61814
14.931	-1.16643	-.17874	-1.18627	-.17874	-.58215
14.932	-1.14665	-.17776			-.58134
15.000	-1.19833	-.16842	-1.29541	-.08175	-.55657
15.125	-1.21837	-.15239	-1.27453	.09551	-.44765
15.250	-1.23650	-.13789	-1.27142	.27398	-.35823
15.326	-1.24679	-.12664	-1.24637	.12664	-.30065
15.375	-1.23955	.16036			-.26323
15.500	-1.21250	.26587			-.16560
15.625	-1.17325	.36135			-.06632
15.750	-1.12235	.45201			.03562
15.875	-1.06048	.53710			.13323
16.000	-.98835	.61594			.23151
16.125	-.90677	.68788			.32747
16.250	-.81662	.75235			.42017
16.375	-.71903	.80885			.50866
16.500	-.61433	.85693			.59207
16.625	-.50515	.89623			.66957
16.750	-.39115	.92643			.74038
16.875	-.27393	.94744			.80378
17.000	-.15468	.95901			.85916
17.125	-.03457	.96115			.90595
17.250	.08521	.95689			.94370
17.375	.20351	.93735			.97201
17.500	.31918	.91175			.97061
17.625	.43109	.87753			.97931
17.750	.53817	.83460			.99203
17.875	.63940	.78385			.99677
18.000	.73582	.72566			.96565
OMEGA = .9	INTERVAL = .0011111111	LOAD INERTIA = .5			
10.110	1.14755	.20685	1.13815	.02128	.32005
10.221	1.17155	.18926	1.13007	-.16648	.22389

86